IMA Journal of Numerical Analysis (2012) **32**, 1375–1403
doi:10.1093/imanum/drr026
Advance Access publication on January 25, 2012

Design and convergence analysis for an adaptive discretization of the heat equation

CHRISTIAN KREUZER
Fakultät für Mathematik, Universität Bochum, Universitätsstraße 150, 44801 Bochum, Germany
christian.kreuzer@rub.de

CHRISTIAN A. MÖLLER
Institut für Mathematik, Universität Augsburg, Universitätsstraße 14, 86159 Augsburg, Germany
c.moeller@math.uni-augsburg.de

ALFRED SCHMIDT*
Zentrum für Technomathematik, Universität Bremen, Bibliothekstraße 1, 28359 Bremen, Germany
*Corresponding author: schmidt@math.uni-bremen.de

AND

KUNIBERT G. SIEBERT
Institut für Angewandte Analysis und Numerische Simulation, Universität Stuttgart, Pfaffenwaldring 57, D-70569 Stuttgart, Germany
kg.siebert@ians.uni-stuttgart.de

[Received on 14 December 2010; revised on 25 May 2011]

We derive an algorithm for the adaptive approximation of solutions to parabolic equations. It is based on adaptive finite elements in space and the implicit Euler discretization in time with adaptive time-step sizes. We prove that, given a positive tolerance for the error, the adaptive algorithm reaches the final time with a space–time error between continuous and discrete solution that is below the given tolerance. Numerical experiments reveal a more than competitive performance of our algorithm ASTFEM (adaptive space–time finite element method).

Keywords: adaptive finite elements; parabolic problems; convergence analysis.

1. Introduction

We analyse the adaptive approximation of solutions to linear parabolic partial differential equations by finite elements. More precisely, we consider equations of the type

$$\begin{aligned} \partial_t u + \mathcal{L}u &= f && \text{in } \Omega \times (0,T), \\ u &= 0 && \text{on } \partial\Omega \times (0,T), \\ u(\cdot,0) &= u_0 && \text{in } \Omega, \end{aligned} \tag{1.1}$$

where Ω is a bounded polyhedral domain in $\mathbb{R}^d$, where $d \in \mathbb{N}$, $\mathcal{L}u = -\operatorname{div} \mathbf{A}\nabla u + cu$ is a symmetric second-order elliptic operator with respect to space and $\partial_t u = \frac{\partial u}{\partial t}$ denotes the partial derivative with respect to time. In the simplest setting $\mathcal{L} = -\Delta$, (1.1) becomes the heat equation. Precise assumptions on data are given in Section 2.1 below.

We discretize (1.1) using adaptive finite elements in space combined with the implicit Euler scheme in time employing adaptively chosen time-step sizes. The conforming finite element spaces are piecewise

polynomials of fixed degree over a simplicial triangulation of the domain Ω. In each single time step we reduce or enlarge the local time-step size and refine and coarsen the underlying triangulation. The time-discrete finite element functions U_n, where $n = 0, \ldots, N$, are computed with a classical time-stepping scheme, i.e., they are computed inductively starting with an approximation U_0 of the initial values u_0. The exact definition of the discretization and the notion of a conforming approximation U to u, which is constructed from the discrete values U_n, are given in Section 2.2.

One important ingredient of an adaptive method is an *a posteriori* error estimator giving a computable bound for the true error. Numerous such estimators for various error notions can be found in the literature; see, e.g., Eriksson & Johnson (1991, 1995) and Lakkis & Makridakis (2006). For our purpose we adapt the residual-based estimator derived by Verfürth (2003) for the heat equation to our problem in Section 3.1. This estimator has also been considered by Chen & Feng (2004). The estimator is constructed from five indicators: an indicator for the initial error, indicators for the temporal and spatial error, a coarsening error indicator and one indicator controlling a so-called consistency error. The adaptation of the time-step size uses information from the indicators for the temporal error and the consistency error. The adaptation of the spatial triangulation is based on refinement by bisection using information from the indicators for the spatial error and coarsening error.

The objective of this article is the design and a detailed convergence analysis of an adaptive finite element method for solving (1.1). This means that we design an adaptive algorithm such that the final time T is reached in a finite number N of time steps with a total space–time error that is below a given tolerance $\mathrm{TOL} > 0$.

By now the convergence and optimality of adaptive methods for inf–sup and coercive problems respectively, are well established (Dörfler, 1996; Morin *et al.*, 2000, 2002, 2003, 2008; Binev *et al.*, 2004; Chen & Feng, 2004; Mekchay & Nochetto, 2005; Stevenson, 2007; Cascón *et al.*, 2008; Diening & Kreuzer, 2008; Siebert, 2011; Kreuzer & Siebert, 2011); compare also the overview article by Nochetto *et al.* (2009). Recently, Schwab & Stevenson (2009) proved optimal computational complexity of an adaptive wavelet method for parabolic problems enforcing coercivity by a least squares formulation.

In contrast to the situation for above mentioned problems, the convergence analysis of adaptive finite element discretizations for time-dependent problems is still in its infancy. To the best of our knowledge, there exists only one preliminary result by Chen & Feng (2004). Their adaptive procedure for a single time step is a two-step procedure. Starting with the grid from the old time step, they only allow for refinement of the spatial grid and a reduction of the time-step size in the first phase. This process is iterated until a suitable tolerance is reached. In the second phase they perform *one* single coarsening step for the spatial grid based on another tolerance $\mathrm{TOL}_{\mathrm{coarse}}$ and enlarge the time-step size as an initial guess for the next time step if appropriate.

The main result of Chen and Feng may be summarized as follows: the adaptive iteration in each single time step terminates within finitely many iterations and the space–time error is always bounded by the given tolerance TOL up to a coarsening error.

In proving termination of the adaptive iteration they show that for each single time step n there exists a minimal time-step size $\tau_n^* > 0$ that is a lower bound for the adaptive time-step size τ_n selected by the adaptive method. The accepted time-step size τ_n is therefore constructed in a finite number of iterations and then stays fixed. In the remaining iteration the adaptive process therefore reduces to an adaptive approximation of a solution to an elliptic equation by finite elements. Termination of this iteration is then a consequence of the aforementioned results for stationary problems.

Although being the first convergence result for adaptive finite elements for time-dependent problems, the result by Chen and Feng bears two weak points. Firstly, it does not guarantee that the final time T is reached, i.e., the adaptively generated sequence of time instances $\{t_n\}_{n\geqslant 0}$ may not be finite and such

that $t_n \to T_* < T$ as $n \to \infty$. This is a consequence of the construction of τ_n^* with a dependence on n not allowing for a uniform lower bound. Secondly, the coarsening error is bounded by the given tolerance $\mathrm{TOL}_{\mathrm{coarse}}$ times a constant that depends on the ratio of the local mesh size squared and the local time-step size. Such a dependence is highly undesirable and stems from a mismatch of the norm for the space–time error and the one used for controlling the coarsening error.

We improve on the result of Chen and Feng by showing that a suitably modified algorithm always reaches the final time. Moreover, the space–time error is below the given tolerance $\mathrm{TOL} > 0$. One important ingredient used by the algorithm is a *uniform in time* bound for the energy of the discrete solution in terms of the right-hand side f and the discrete initial values U_0, which is derived in Section 3.2. From this bound and the tolerance TOL one can compute *a priori* a suitable minimal time-step size $\tau_* > 0$, which is sufficient for the required accuracy of the discrete solution. Consequently, the reduction of the time-step size τ_n in time step n is aborted whenever it should be reduced below τ_*. After this point, the adaptive procedure is again the adaptive approximation of a solution to a stationary problem. Termination of this iteration follows with standard results for elliptic problems. The uniform lower bound $\tau_n \geqslant \tau_*$ in turn implies that the final time T is reached within a finite number of time steps.

Allowing for (locally) coarser grids between different time steps is necessary when dealing with adaptive finite elements for unsteady problems. Unfortunately, such coarsening may increase the energy of the discrete solution, which in turn spoils the crucial energy estimate. Consequently, the adaptive method has to control a possible increase of energy. Permitting a coarsening step just at the end of each time step, as in the algorithm of Chen and Feng, it is impossible to simultaneously control the coarsening error and an increase of energy.

Therefore, we perform one single coarsening step at the *beginning* of each time step and then only allow for refinement. This is the basic idea of our algorithm ASTFEM (adaptive space–time finite element method), which is presented in detail in Section 3.3. A practical drawback of this approach is the fact that one simultaneously needs two grids, one for the old and one for the current time step. This was avoided in the algorithm of Chen and Feng, where only the grid of the current time step is needed. We overcome this implementational problem by using the multi-mesh tools derived in Schmidt (2003a,b). A drawback in the analysis is the fact that the finite element spaces of two subsequent time steps are no longer nested, which complicates the analysis.

The advantage of our approach is twofold. Firstly, the coarsening error is controlled in a natural norm and, as a consequence, coarsening does not spoil the final bound for the space–time error. Secondly, an increase of energy can be reduced *a posteriori* by appropriate refinements, leading to a uniform energy bound, which is the key for computing the minimal time-step size τ_*. This in turn ensures that the time-stepping scheme reaches the final time in a finite number of steps. The detailed convergence analysis is given in Section 4.

We conclude the paper in Section 5 by comments on the implementation in the finite element toolbox ALBERTA (Schmidt & Siebert, 2005; Schmidt *et al.*, 2005) and some numerical experiments. In particular, we give a short description of the coarsening strategy used. The experiments show a more than competitive performance of our algorithm ASTFEM.

2. The continuous and discrete problems

We state the continuous problem together with the assumptions on data. Then we describe the discretization by adaptive finite elements in space combined with the implicit Euler scheme in time.

2.1 *The weak formulation*

For $d \in \mathbb{N}$, let $\Omega \subset \mathbb{R}^d$ be a bounded polyhedral domain that is triangulated by some conforming triangulation $\mathcal{G}_{\text{init}}$. We denote by $H^1(\Omega)$ the Sobolev space of functions in $L^2(\Omega)$ whose first derivatives are in $L^2(\Omega)$ and we let $\mathbb{V} := H_0^1(\Omega)$ be the space of functions in $H^1(\Omega)$ with vanishing trace on $\partial\Omega$. For any measurable set ω and $n \in \mathbb{N}$ we denote by $\|\cdot\|_\omega$ the $L^2(\omega;\mathbb{R}^n)$ norm, whence $\|v\|^2_{H^1(\Omega)} = \|v\|^2_\Omega + \|\nabla v\|^2_\Omega$.

We suppose that the data of (1.1) satisfy the following properties: $\mathbf{A}$: $\Omega \to \mathbb{R}^{d\times d}$ is piecewise Lipschitz over $\mathcal{G}_{\text{init}}$ and is symmetric positive definite with eigenvalues bounded by $0 < a_* \leqslant a^* < \infty$, i.e.,

$$a_*|\boldsymbol{\xi}|^2 \leqslant \mathbf{A}(x)\boldsymbol{\xi}\cdot\boldsymbol{\xi} \leqslant a^*|\boldsymbol{\xi}|^2 \quad \text{for all } \boldsymbol{\xi} \in \mathbb{R}^d, \ \ x \in \Omega, \tag{2.1}$$

$c \in L^\infty(\Omega)$ is non-negative, i.e., $c \geqslant 0$ in Ω, $f \in H^1((0,T);L^2(\Omega))$; this means that $f, \partial_t f \in L^2(\Omega\times(0,T))$, and $u_0 \in L^2(\Omega)$. The regularity assumptions on $\mathbf{A}$ and f can be relaxed for the weak formulation. The residual error estimator of Section 3.1 requires the piecewise smoothness of $\mathbf{A}$ and the convergence proof in Section 4 utilizes the additional regularity of f in time.

We next turn to the weak formulation of (1.1); compare with Evans (1998, Chapter 7). Let $\mathcal{B}$: $\mathbb{V}\times\mathbb{V}\to\mathbb{R}$ be the symmetric bilinear form associated with the weak form of the elliptic operator $\mathcal{L}$, i.e.,

$$\mathcal{B}[w,\,v] := \int_\Omega \mathbf{A}\nabla v\cdot\nabla w + cvw\,\mathrm{d}x \quad \text{for all } v, w \in \mathbb{V}.$$

Recalling the Poincaré–Friedrichs inequality, $\|v\|_\Omega \leqslant C(d,\Omega)\|\nabla v\|_\Omega$ for all $v \in \mathbb{V}$ (Gilbarg & Trudinger 2001, p. 158), we deduce from (2.1) that $\mathcal{B}$ is a scalar product on $\mathbb{V}$ with induced norm

$$|\!|\!|v|\!|\!|^2_\Omega := \mathcal{B}[v,\,v] = \int_\Omega \mathbf{A}\nabla v\cdot\nabla v + cv^2\,\mathrm{d}x \quad \text{for all } v \in \mathbb{V}.$$

This *energy norm* is equivalent to the H^1-norm and we will be using the energy norm $|\!|\!|\cdot|\!|\!|_\Omega$ in the subsequent analysis. We denote the restriction of the energy norm to some subset $\omega \subset \Omega$ by $|\!|\!|\cdot|\!|\!|_\omega$. We let $\mathbb{V}^* := H^{-1}(\Omega)$ be the topological dual space of $H_0^1(\Omega)$ equipped with the operator norm $|\!|\!|g|\!|\!|_* := \sup_{v\in\mathbb{V}} \frac{\langle g,\,v\rangle}{|\!|\!|v|\!|\!|_\Omega}$.

The parabolic solution space

$$\mathbb{W}(0,T) := \{u \in L^2(0,T;\mathbb{V}) \,|\, \partial_t u \in L^2(0,T;\mathbb{V}^*)\}$$

is a Banach space endowed with the norm

$$\|v\|^2_{\mathbb{W}(0,T)} = \int_0^T |\!|\!|\partial_t v|\!|\!|^2_* + |\!|\!|v|\!|\!|^2_\Omega\,\mathrm{d}t, \quad v \in \mathbb{W}(0,T),$$

and continuously embeds into $C^0([0,T];L^2(\Omega))$ (see, e.g., Evans, 1998, Chapter 5, Theorem 3).

After this preparation we are in a position to state the weak form of (1.1). A function $u \in \mathbb{W}(0,T)$ is a weak solution to (1.1) if it satisfies for a.e. $t \in (0,T)$

$$\langle \partial_t u(t),\,v\rangle + \mathcal{B}[u(t),\,v] = \langle f(t),\,v\rangle_\Omega \quad \text{for all } v \in \mathbb{V}, \tag{2.2a}$$

$$u(0) = u_0. \tag{2.2b}$$

Hereafter, $\langle\cdot,\cdot\rangle_\Omega$ denotes the $L^2(\Omega)$ scalar product. Since the operator $\mathcal{L}$ is elliptic, problem (2.2) admits for any $f \in L^2(0,T;L^2(\Omega))$ and $u_0 \in L^2(\Omega)$ a unique weak solution; compare with Evans (1998, Chapter 7, Theorems 3 and 4).

2.2 *The discrete problem*

For the discretization of (2.2) we use adaptive finite elements in space and the implicit Euler scheme with adaptive time-step sizes in time.

2.2.1 *Adaptive grids and time steps.* For the adaptive space discretization we restrict ourselves to simplicial grids and local refinement by bisection; compare with Bänsch (1991), Kossaczký (1994), Maubach (1995), Traxler (1997) as well as Schmidt & Siebert (2005), Nochetto *et al.* (2009) and the references therein. To be more precise, refinement is based on the initial conforming triangulation $\mathcal{G}_{\text{init}}$ of Ω and a procedure `REFINE` with the following properties. Given a conforming triangulation $\mathcal{G}$ and a subset $\mathcal{M} \subset \mathcal{G}$ of *marked elements*,

$$\texttt{REFINE}(\mathcal{G},\mathcal{M})$$

outputs a conforming refinement $\mathcal{G}_+$ of $\mathcal{G}$ such that all elements in $\mathcal{M}$ are bisected at least once. In general, additional elements are refined in order to ensure conformity. The input $\mathcal{G}$ can either be $\mathcal{G}_{\text{init}}$ or the output of a previous application of `REFINE`. The class of all conforming triangulations that can be produced from $\mathcal{G}_{\text{init}}$ by `REFINE` is denoted by $\mathbb{G}$. For $\mathcal{G} \in \mathbb{G}$, we call $\mathcal{G}_+ \in \mathbb{G}$ a *refinement* of $\mathcal{G}$ if $\mathcal{G}_+$ is produced from $\mathcal{G}$ by a finite number of applications of `REFINE` and we denote this by $\mathcal{G} \leqslant \mathcal{G}_+$ or $\mathcal{G}_+ \geqslant \mathcal{G}$. Conversely, any $\mathcal{G}_- \in \mathbb{G}$ with $\mathcal{G}_- \leqslant \mathcal{G}$ is called a *coarsening* of $\mathcal{G}$.

Throughout the discussion we only deal with conforming grids; this means that whenever we refer to some triangulations $\mathcal{G}$, $\mathcal{G}_+$ and $\mathcal{G}_-$, we tacitly assume $\mathcal{G},\mathcal{G}_+,\mathcal{G}_- \in \mathbb{G}$. Moreover, one key property of the refinement by bisection is uniform shape regularity for any $\mathcal{G} \in \mathbb{G}$. This means that all constants depending on the shape regularity are uniformly bounded by a constant depending on $\mathcal{G}_{\text{init}}$.

For the discretization in time we let $0 = t_0 < t_1 < \cdots < t_N = T$ be a partition of $(0,T)$ into subintervals $I_n = [t_{n-1},t_n]$ with corresponding local time-step size $\tau_n := |I_n| = t_n - t_{n-1}$, $n = 1,\dots,N$.

2.2.2 *Space–time discretization* For the spatial discretization we use Lagrange finite elements; that is, for any $\mathcal{G} \in \mathbb{G}$, the finite element space $\mathbb{V}(\mathcal{G})$ consists of all continuous piecewise polynomials of fixed degree $\geqslant 1$ over $\mathcal{G}$ that vanish on $\partial\Omega$. This gives a conforming discretization of $\mathbb{V}$, i.e., $\mathbb{V}(\mathcal{G}) \subset \mathbb{V}$. Moreover, Lagrange finite elements give nested spaces, i.e., $\mathbb{V}(\mathcal{G}) \subset \mathbb{V}(\mathcal{G}_+)$ whenever $\mathcal{G} \leqslant \mathcal{G}_+$. For the time discretization we use the implicit Euler scheme.

For $n \geqslant 0$ we denote by $\mathcal{G}_n$ the actual grid at time t_n and let $\mathbb{V}_n = \mathbb{V}(\mathcal{G}_n)$ be the corresponding finite element space. For $\mathcal{G} \in \mathbb{G}$ we denote by $\Pi_{\mathcal{G}}\colon L^2(\Omega) \to \mathbb{V}(\mathcal{G})$ the L^2-projection onto $\mathbb{V}(\mathcal{G})$ and set $\Pi_n := \Pi_{\mathcal{G}_n}$. Furthermore, for any interval I with $0 < |I| < \infty$ we let

$$\fint_I f(t)\,\mathrm{d}t := \frac{1}{|I|}\int_I f(t)\,\mathrm{d}t$$

be the mean value of f over I. In particular, we use $f_n := \fint_{I_n} f(t)\,\mathrm{d}t$ as a time discretization of f on I_n.

We construct a conforming approximation $U \in \mathbb{W}(0,T)$ to the exact solution u as follows. We start with a suitable initial refinement $\mathcal{G}_0 \in \mathbb{G}$ and $U_0 = \Pi_0 u_0 \in \mathbb{V}(\mathcal{G}_0)$ as an approximation of the

initial value u_0. Principally, any suitable interpolation operator could be used instead of Π_0. We then inductively compute for $n > 0$ on a suitable grid $\mathcal{G}_n \in \mathbb{G}$ a solution U_n to the elliptic problem

$$U_n \in \mathbb{V}_n\colon \frac{1}{\tau_n}\langle U_n - U_{n-1},\, V\rangle_\Omega + \mathcal{B}[U_n,\, V] = \langle f_n,\, V\rangle_\Omega \quad \text{for all } V \in \mathbb{V}_n. \tag{2.3}$$

From these pointwise approximations U_n to $u(t_n)$ we finally define the continuous, piecewise affine function

$$U(t) := \frac{t - t_{n-1}}{\tau_n} U_n + \frac{t_n - t}{\tau_n} U_{n-1} \quad \text{for } t \in I_n,\ \ n = 1, \dots, N. \tag{2.4}$$

Continuity of U in time in combination with $U_n \in \mathbb{V}_n \subset \mathbb{V}$ for $n = 0, \dots, N$ then implies $U \in \mathbb{W}(0, T)$.

Note that we do not ask $\mathcal{G}_n$ to be a refinement of $\mathcal{G}_{n-1}$ and vice versa. As a consequence, in general neither $\mathcal{G}_n \leqslant \mathcal{G}_{n-1}$ nor $\mathcal{G}_{n-1} \leqslant \mathcal{G}_n$ holds, i.e., $\mathcal{G}_n$ may be finer than $\mathcal{G}_{n-1}$ in parts of the domain and coarser in other parts. In such a situation, we have $\mathbb{V}_{n-1} \not\subset \mathbb{V}_n$ and $\mathbb{V}_n \not\subset \mathbb{V}_{n-1}$, which implies that $U(t) \notin \mathbb{V}_{n-1}$ and $U(t) \notin \mathbb{V}_n$ for $t \in (t_{n-1}, t_n)$. Nevertheless, in any case, $U(t)$ is a finite element function since $U(t) \in \mathbb{V}(\mathcal{G}_{n-1} \oplus \mathcal{G}_n)$, where $\mathcal{G}_{n-1} \oplus \mathcal{G}_n$ is the smallest common refinement of $\mathcal{G}_{n-1}$ and $\mathcal{G}_n$, which we call an *overlay*.

3. The adaptive space–time finite element method (ASTFEM)

In this section we derive our adaptive algorithm ASTFEM. We start with recalling an estimator for (1.1). We then describe how tolerances for the single time steps are constructed in standard time-stepping schemes and shed some light on the intrinsic difficulties that arise from this procedure. We finally present the adaptive algorithm ASTFEM and describe its modules in detail.

3.1 *Error estimation*

One important ingredient for the adaptive method is an *a posteriori* error estimator that gives a computable bound for the true error in terms of the discrete solution and data of the problem. We adapt the residual estimator derived by Verfürth (2003) for the heat equation to our problem (1.1).

We start by defining some error indicators that build up the estimator. In doing this, we use the constants $C_0 = 3$, $C_{c\tau} = 5$, $C_f = 15C(\Omega)$, where $C(\Omega)$ is the Poincaré–Friedrichs constant of Ω, and a suitably chosen constant $C_{\mathcal{G}} > 0$; compare (3.4) and Remark 3.2 below. For $\mathcal{G} \in \mathbb{G}$ and $v \in \mathbb{V}$, we then define

$$\mathcal{E}_0^2(v, \mathcal{G}) := C_0 \|v - \Pi_0 v\|_\Omega^2 \tag{3.1a}$$

for estimating the initial error. To estimate the space–time error we use the following indicators that are defined for $v, w \in H_0^1(\Omega)$, $f \in L^2(0, T; L^2(\Omega))$, $t, \tau, t + \tau \in (0, T)$, $V \in \mathbb{V}(\mathcal{G})$, $E \in \mathcal{G}$ and $g \in L^2(\Omega)$ as

$$\mathcal{E}_f^2(f, t, \tau) := C_f \inf_{\bar f \in L^2(\Omega)} \fint_{(t,t+\tau)} \|f - \bar f\|_\Omega^2 \,\mathrm{d}s, \tag{3.1b}$$

$$\mathcal{E}_{c\tau}^2(v, w, \mathcal{G}) := C_{c\tau} |\!|\!| v - w |\!|\!|_\Omega^2, \tag{3.1c}$$

$$\mathcal{E}_{\mathcal{G}}^2(V, w, \tau, g, \mathcal{G}, E) := C_{\mathcal{G}} \left(h_E^2 \left\| \frac{1}{\tau}(V - w) + \mathcal{L}V - g \right\|_E^2 + h_E \|J(V)\|_{\partial E}^2 \right). \tag{3.1d}$$

Hereby, we denote by $J(V)$ the jump of the normal flux $\mathbf{A}\nabla V \cdot \boldsymbol{n}$ across an interior side S and we set $J(V) = 0$ on a boundary side S. The mesh size of an element $E \in \mathcal{G}$ is given by $h_E := |E|^{1/d}$ and the mesh-size function $h_{\mathcal{G}}\colon \Omega \to \mathbb{R}^+$ is the piecewise constant function with $h_{\mathcal{G}|E} = h_E$, $E \in \mathcal{G}$.

We briefly comment on the different indicators. The indicator $\mathcal{E}_f$ bounds the consistency error that naturally arises from using f_n in (2.3). The infimum in $\mathcal{E}_f$ is attained for the mean value $\bar{f} = \fint_t^{t+\tau} f \,\mathrm{d}s$.

The indicator $\mathcal{E}_{c\tau}$ is a *combined* coarsening–time error indicator. It can be naturally split into

$$\mathcal{E}_c^2(w, \mathcal{G}) := \sum_{E\in\mathcal{G}} \mathcal{E}_c^2(w, \mathcal{G}, E) := C_{c\tau} \sum_{E\in\mathcal{G}} |\!|\!| \Pi_{\mathcal{G}} w - w |\!|\!|_E^2 \tag{3.2a}$$

and

$$\mathcal{E}_\tau^2(v, w, \mathcal{G}) := C_{c\tau} |\!|\!| v - \Pi_{\mathcal{G}} w |\!|\!|_\Omega^2. \tag{3.2b}$$

Indeed, using $v = U_n$, $w = U_{n-1}$ and $\mathcal{G} = \mathcal{G}_n$, the indicator $\mathcal{E}_c^2(U_{n-1}, \mathcal{G}_n) = C_{c\tau} |\!|\!| \Pi_n U_{n-1} - U_{n-1} |\!|\!|_\Omega^2$ is an obvious measure for the coarsening error and $\mathcal{E}_\tau^2(U_n, U_{n-1}, \mathcal{G}_n) = C_{c\tau} |\!|\!| U_n - \Pi_n U_{n-1} |\!|\!|_\Omega^2$ is the coarsening-adjusted classical temporal error indicator. Note that using $\mathcal{E}_{c\tau}^2(v, w, \mathcal{G})$ in the estimator gives a better bound than the estimate $\mathcal{E}_{c\tau}^2(v, w, \mathcal{G}) \leqslant 2\mathcal{E}_c^2(v, \mathcal{G}) + 2\mathcal{E}_\tau^2(v, w, \mathcal{G})$. At this stage, we could also use any interpolant of w instead of $\Pi_{\mathcal{G}} w$. The particular choice of the L^2-projection $\Pi_{\mathcal{G}} w$ will become important later; compare with Proposition 3.6 below.

Finally, $\mathcal{E}_{\mathcal{G}}$ is an indicator for the spatial error. For given $\bar{f}, g \in L^2(\Omega)$ and $\tau > 0$ the sum of indicators $\mathcal{E}_{\mathcal{G}}^2(U_\tau, g, \tau, \bar{f}, \mathcal{G}, E)$ gives an estimator $\mathcal{E}_{\mathcal{G}}^2(U_\tau, g, \tau, \bar{f}, \mathcal{G})$ for the *elliptic* problem

$$\frac{1}{\tau} u_\tau + \mathcal{L} u_\tau = \frac{1}{\tau} g + \bar{f}. \tag{3.3}$$

More precisely, if $u_\tau \in \mathbb{V}$ is the weak solution to (3.3) and $U_\tau \in \mathbb{V}(\mathcal{G})$ its Ritz approximation, then

$$|\!|\!| U_\tau - u_\tau |\!|\!|_\Omega^2 \leqslant \frac{1}{15} \mathcal{E}_{\mathcal{G}}^2(U_\tau, g, \tau, \bar{f}, \mathcal{G}) := \frac{1}{15} \sum_{E\in\mathcal{G}} \mathcal{E}_{\mathcal{G}}^2(U_\tau, g, \tau, \bar{f}, \mathcal{G}, E). \tag{3.4}$$

Hereby we assume that the constant $C_{\mathcal{G}}$, which enters into the definition of the indicators, is chosen appropriately. Note that $C_{\mathcal{G}}$ depends on the globally smallest eigenvalue a_* of $\mathbf{A}$ and on the shape regularity of $\mathbb{G}$ but not on the parameter τ; compare with Verfürth (1996) and Ainsworth & Oden (2000). We would like to remark that $\mathcal{E}_{\mathcal{G}}$ is not a robust estimator with respect to τ for the specific energy error of the elliptic problem (3.3) in that the constant of the corresponding lower bound depends on τ; compare with Verfürth (1998) and Remark 3.3 below.

Using these indicators we obtain the following result, which can be found in Verfürth (2003, Theorem 1.1).

THEOREM 3.1 (*A posteriori* ERROR ESTIMATE) If u is the solution to (2.2) and if U is the discrete solution from (2.4), then there holds for any $m = 1, \ldots, N$ the upper bound

$$\|U - u\|_{\mathbb{W}(0,t_m)}^2 \leqslant \mathcal{E}_0^2(u_0, \mathcal{G}_0) + \sum_{n=1}^{m} \tau_n \Big(\mathcal{E}_{\mathcal{G}}^2(U_n, U_{n-1}, \tau_n, f_n, \mathcal{G}_n) + \mathcal{E}_{c\tau}^2(U_n, U_{n-1}, \mathcal{G}_n) + \mathcal{E}_f^2(f, t_{n-1}, \tau_n) \Big).$$

Some remarks about this result are in order.

REMARK 3.1 (EXPLICIT CONSTANTS) The values $C_0 = 3$, $C_{c\tau} = 5$, $C_f = 15C(\Omega)$ and the constant $\frac{1}{15}$ in (3.4) can be traced explicitly. To that end, one first employs the basic bound

$$\|U - u\|^2_{\mathbb{W}(0,t_m)} \leqslant 3\|U_0 - u_0\|^2_{\Omega} + 5 \int_0^{t_m} |\!|\!| \mathcal{R}(U) |\!|\!|^2_* \, \mathrm{d}t$$

of the error by the residual $\mathcal{R}(U) := \partial_t U + \mathcal{L}U - f$; compare with Verfürth (2003, Lemma 4.1). Note that slightly different constants show up since Verfürth includes the $\|\cdot\|_{L^\infty(0,t_m)}$ norm in the definition of the $\|\cdot\|_{\mathbb{W}(0,t_m)}$ norm. In a second step one has to split the residual $\mathcal{R}(U)$ into three parts: the residual related to the consistency error, the spatial residual and the temporal residual; compare with Verfürth (2003, Section 6). This splitting of $|\!|\!| \mathcal{R}(U) |\!|\!|^2_*$ gives rise to an additional factor 3 by Young's inequality.

REMARK 3.2 (ROBUST ESTIMATOR FOR THE ELLIPTIC PROBLEM) The estimator $\mathcal{E}_{\mathcal{G}}$ for the elliptic problem (3.3) is not robust in the case of dominant reaction $c \gg 1$ or jumping coefficients $\mathbf{A}$. In the first case one should replace $\mathcal{E}_{\mathcal{G}}$ by the robust estimator for the elliptic problem stated in Verfürth (1998). This in turn gives the estimator for the parabolic problem derived in Verfürth (2005). In the latter case one could resort to the estimator for the elliptic problem given by Petzoldt (2001, 2002) which turns out to be robust if the jumps are quasi-monotone with respect to the triangulation. For the sake of clarity, we restrict ourselves to the estimator $\mathcal{E}_{\mathcal{G}}$ as stated above. We emphasize that using the other estimators does not affect the results of this paper since the convergence result for the elliptic problem of Morin *et al.* (2008) and Siebert (2011) stated in Proposition 4.2 below for our situation also holds true for the robust estimators.

REMARK 3.3 (UPPER AND LOWER BOUND) Besides the upper bound as stated in Theorem 3.1, Verfürth has also derived a lower bound up to oscillation; compare with Verfürth (2003, Theorem 1.1). Both constants are independent of the mesh size and the time-step size. We comment on a slight difference of the estimator stated in Theorem 3.1 and the one by Verfürth. For ease of discussion, we consider the heat equation, i.e., $\mathcal{L} = -\Delta$. In this case, oscillation in the lower bound reduces to $\|f - f_{\mathcal{G}_n,\tau_n}\|_{L^2(I_n,H^{-1}(\Omega))}$, with a suitable space–time approximation $f_{\mathcal{G}_n,\tau_n}$ of f on the interval I_n.

The spatial estimator of Verfürth $\mathcal{E}_{\mathcal{G}}$ utilizes the overlay $\mathcal{G}_n \oplus \mathcal{G}_{n-1}$ instead of $\mathcal{G}_n$. This is a necessity when analysing the temporal discretization with a θ-scheme, where $\theta = 1$ is the implicit Euler discretization and $\theta = \frac{1}{2}$ is the Crank–Nicholson scheme. Here one has to estimate $\mathcal{L}(\theta U_n + (1-\theta)U_{n-1})$, which involves evaluating the differential operator on the finite element functions U_n existing on $\mathcal{G}_n$ and U_{n-1} defined on $\mathcal{G}_{n-1}$. As a consequence, the constant of the spatial estimator additionally depends on a constant $C(\mathcal{G}_{n-1}, \mathcal{G}_n)$ that relates the local mesh size of coarsened elements in $\mathcal{G}_n$ compared to the local mesh size in $\mathcal{G}_{n-1}$. It is assumed that this constant is uniformly bounded by a so-called transition condition. The constant in the lower bound of the space–time error and estimator is independent of any constant $C(\mathcal{G}_{n-1}, \mathcal{G}_n)$.

When only dealing with the implicit Euler discretization, the spatial estimator can be defined on $\mathcal{G}_n$ since one only has to estimate the term $\mathcal{L}U_n$. Accordingly, the upper bound is robust with respect to any coarsening of $\mathcal{G}_n$ relative to $\mathcal{G}_{n-1}$. Striking for the same oscillation term in the lower bound as above for the estimator of Theorem 3.1, one has to use cut-off functions with support inside elements of $\mathcal{G}_n \oplus \mathcal{G}_{n-1}$. Consequently, the constant of the lower bound depends on $C(\mathcal{G}_{n-1}, \mathcal{G}_n)$. Allowing for an oscillation term that also may depend on U_{n-1}/τ_n one can use cut-off functions with support inside elements of $\mathcal{G}_n$ and the constant in the lower bound becomes independent of $C(\mathcal{G}_{n-1}, \mathcal{G}_n)$. Note that in coarsened regions of $\mathcal{G}_n$, U_{n-1} is a nonsmooth function.

In any case, if $\mathcal{G}_n$ is (locally) quite coarse compared to $\mathcal{G}_{n-1}$, the constant of the upper bound is independent of $C(\mathcal{G}_{n-1}, \mathcal{G}_n)$. Nevertheless, we may drastically overestimate the true error since either

$C(\mathcal{G}_{n-1}, \mathcal{G}_n)$ is large or the part of the oscillation related to U_{n-1}/τ_n is large. In view of this observation it may be recommended to also require a transition condition between grids of subsequent time steps when using the Euler discretization.

3.2 *Motivation and design of the adaptive algorithm*

We next want to design an algorithm that is guaranteed to construct an adaptive approximation U to the true solution u of (2.2) on the complete time interval $(0, T)$ with an error $\|u - U\|_{\mathbb{W}(0,T)}$ below a given tolerance.

In order to do that, let us first review the usual, 'classical' adaptive finite element time-stepping algorithm for parabolic problems used in theory and practice (compare, e.g., Chen & Feng, 2004; Schmidt & Siebert, 2005). Keeping in mind the goal of proving termination of the adaptive loops (in each time-step and over the complete time interval), we analyse the ingredients of the adaptive algorithm in order to overcome the arising difficulties by appropriate modifications of the classical method.

3.2.1 *Review of the classical adaptive algorithm.* In the classical approach of an adaptive time-stepping scheme, the quantities $U_0, \ldots, U_N$ are computed inductively. In this process both the current grid and the current time-step size are adapted according to error indicators. Therefore, each single time step is an adaptive loop that constructs a suitable final mesh $\mathcal{G}_n$ and final time-step size τ_n. The adaptive process should be such that having reached the final time T we have the bound

$$\|U - u\|_{\mathbb{W}(0,T)} \leqslant \mathrm{TOL}, \tag{3.5}$$

where $\mathrm{TOL} > 0$ is some given tolerance for the space–time error.

To ensure (3.5), it is customary to split the given tolerance TOL into three parts TOL_0, TOL_f and $\mathrm{TOL}_{\mathcal{G}_\tau}$ such that

$$\mathrm{TOL}_0^2 + T\,\mathrm{TOL}_f^2 + T\,\mathrm{TOL}_{\mathcal{G}_\tau}^2 = \mathrm{TOL}^2 \tag{3.6}$$

and to demand that the adaptive algorithm guarantees the bounds

$$\mathcal{E}_0^2(u_0, \mathcal{G}_0) \leqslant \mathrm{TOL}_0^2 \tag{3.7a}$$

in the construction of $\mathcal{G}_0$ and

$$\mathcal{E}_f^2(f, t_n, \tau_n) \leqslant \mathrm{TOL}_f^2, \tag{3.7b}$$

$$\mathcal{E}_{\mathcal{G}}^2(U_n, U_{n-1}, \tau_n, f_n, \mathcal{G}_n) + \mathcal{E}_{c\tau}^2(U_n, U_{n-1}, \mathcal{G}_n) \leqslant \mathrm{TOL}_{\mathcal{G}_\tau}^2 \tag{3.7c}$$

when adaptively constructing the grids $\mathcal{G}_n$ and time-step sizes τ_n, where $n \geqslant 1$. Assuming that the algorithm reaches the final time T in time step N, one directly obtains from Theorem 3.1 the bound

$$\|u - U\|_{\mathbb{W}(0,T)}^2 \leqslant \mathrm{TOL}_0^2 + \sum_{n=1}^{N} \tau_n \left(\mathrm{TOL}_{\mathcal{G}_\tau}^2 + \mathrm{TOL}_f^2\right) = \mathrm{TOL}_0^2 + T\left(\mathrm{TOL}_f^2 + \mathrm{TOL}_{\mathcal{G}_\tau}^2\right) = \mathrm{TOL}^2.$$

When analysing such a time-stepping algorithm, the following fundamental questions arise:

(1) Does the adaptive loop of each single time step terminate?
(2) Is the final time T reached, i.e., is there an $N \geqslant 1$ such that $t_N = T$?

If the answers to both questions are positive we conclude that the algorithm reaches the final time with a total number of operations that is bounded and a space–time error that is below tolerance, i.e., (3.5) holds true.

3.2.2 *Accumulation and marking.* A positive answer, however, is nontrivial for the following reason. Suppose for the moment that u_0 is a discrete function in a suitable initial space $\mathbb{V}_0 = \mathbb{V}(\mathcal{G}_0)$ such that we may assume $\mathcal{E}_0^2(u_0, \mathcal{G}_0) = 0$. Interpreting the remaining indicators $\mathcal{E}_f$, $\mathcal{E}_\mathcal{G}$ and $\mathcal{E}_{c\tau}$ as piecewise constant functions in time, we see that the estimator

$$\sum_{n=1}^{N} \tau_n \Big(\mathcal{E}_\mathcal{G}^2(U_n, U_{n-1}, \tau_n, f_n, \mathcal{G}_n) + \mathcal{E}_{c\tau}^2(U_n, U_{n-1}, \mathcal{G}_n) + \mathcal{E}_f^2(f, t_{n-1}, \tau_n) \Big)$$

accumulates in L^2 with respect to time and marking should lead to an equidistribution of these indicators in L^2 with respect to time. This aim yet needs information about the indicators for *all* time instances $t_0, \ldots, t_N$ when insisting on (3.5). In a standard time-stepping scheme information about the indicators for $m > n$ is not available in time step n. Typically, (3.7) is used as a resort to this problem. However, (3.7) aims at an L^∞ in time equidistribution of the piecewise constant functions $\mathcal{E}_f$, $\mathcal{E}_\mathcal{G}$ and $\mathcal{E}_{c\tau}$.

We next shed some light on this problematic mismatch of accumulation and equidistribution by considering the consistency indicator $\mathcal{E}_f$. Using a density argument it is easy to show that for any given $f \in L^2(0, T; L^2(\Omega))$, there exists a partition $0 = t_0 < \cdots < t_N = T$, where $N \in \mathbb{N}$, such that

$$\sum_{n=1}^{N} \tau_n \mathcal{E}_f^2(f, t_{n-1}, \tau_n) = C_f \sum_{n=1}^{N} \int_{I_n} \|f - f_n\|_\Omega^2 \, \mathrm{d}s \leqslant \mathrm{TOL}_f^2.$$

The optimal partition, with the smallest number N of time intervals, is given when the local quantities $\tau_n \mathcal{E}_f^2(f, t_{n-1}, \tau_n)$ are equidistributed. In contrast to this we ask in (3.7b) for

$$\mathcal{E}_f^2(f, t_{n-1}, \tau_n) = \frac{C_f}{\tau_n} \int_{I_n} \|f - f_n\|_\Omega^2 \, \mathrm{d}s \leqslant \mathrm{TOL}_f^2, \quad n = 1, \ldots, N,$$

i.e., we aim at an equidistribution of the terms $\mathcal{E}_f^2(f, t_{n-1}, \tau_n)$. In order that such a bound is true, the terms $\|f - f_n\|_{\Omega \times I_n}^2$ have to compensate for τ_n^{-1}, which requires additional regularity of f in time. Whence for a generic function $f \in L^2(0, T; L^2(\Omega))$ there exists no partition such that (3.7b) is satisfied. A sufficient condition that (3.7b) can be satisfied is given by the following lemma, which is a direct consequence of a standard Poincaré argument.

LEMMA 3.2 If $f \in H^1((0, T); L^2(\Omega))$, then

$$\int_t^{t+\tau} \|f(s) - \bar{f}\|_\Omega^2 \, \mathrm{d}s \leqslant \tau^2 \int_t^{t+\tau} \|\partial_t f(s)\|_\Omega^2 \, \mathrm{d}s \quad \text{for all } t \in [0, T), \quad \tau \in (0, T - t].$$

In particular, for any $\tau \leqslant \mathrm{TOL}_f^2 / (C_f \|\partial_t f\|_{\Omega \times (0,T)}^2)$ we conclude that $\mathcal{E}_f^2(f, t, \tau) \leqslant \mathrm{TOL}_f^2$.

As a result, one finds for any tolerance TOL_f a partition of $(0, T)$ such that the consistency indicator satisfies (3.7b) if $\partial_t f \in L^2(\Omega \times (0, T))$. The lemma even gives a lower bound for the minimal time-step size $\min_n \tau_n$ needed to comply with (3.7b). We would like to mention that requiring less regularity, namely, $\partial_t f \in L^p(\Omega \times (0, T))$ for some $p > 1$, is also sufficient. Usually, the creation of the time instances t_n is subject to restrictions, for instance, any admissible partition $0 = t_0 < \cdots < t_N = T$ is created by recurrent bisection. In such a situation the regularity requirement for f cannot be reduced

below $f \in W_1^1(0,T;L^2(\Omega))$. It is rather easy to construct an example $f \in L^\infty(0,T;L^2(\Omega))$ with $\max_n \mathcal{E}_f^2(f,t_{n-1},\tau_n) \geqslant c > 0$ for any admissible partition.

3.2.3 *Energy estimation.* Summarizing the discussion above, we see that we easily find a partition when equidistributing the local error in its natural norm, whereas equidistribution in a stronger norm requires additional regularity. The consistency indicator $\mathcal{E}_f$ can be handled by assuming sufficient regularity of data f. In contrast to this, the indicators $\mathcal{E}_\mathcal{G}$ and $\mathcal{E}_{c\tau}$ depend on the discrete solution and it is altogether not clear whether the definition of U in Section 2.2 induces the required regularity for these indicators. Of particular interest is the indicator $\mathcal{E}_\tau$ for the time error; the other indicators $\mathcal{E}_\mathcal{G}$ and $\mathcal{E}_c$ can be reduced by appropriate refinements of the spatial grid. The answer to this question for $\mathcal{E}_\tau$ is given by the following bound for the energy of the discrete solution.

PROPOSITION 3.3 (UNIFORM ENERGY ESTIMATE) Assume $N \in \mathbb{N}\cup\{\infty\}$ and arbitrary time instances $t_0,\dots,t_N$ with time-step sizes $\tau_1,\dots,\tau_N > 0$. For $n = 1,\dots,N$ let $U_n \in \mathbb{V}_n$ be the discrete solutions to (2.3).

Then for any $m = 1,\dots,N$ there holds

$$\sum_{n=1}^{m} \frac{1}{\tau_n}\|U_n - \Pi_n U_{n-1}\|_\Omega^2 + |\!|\!| U_n - \Pi_n U_{n-1} |\!|\!|_\Omega^2 + |\!|\!| U_n |\!|\!|_\Omega^2 - |\!|\!| \Pi_n U_{n-1} |\!|\!|_\Omega^2 \leqslant \|f\|_{\Omega\times(0,t_m)}^2.$$

Proof. We set $V := U_n - \Pi_n U_{n-1} \in \mathbb{V}_n$. Recalling that $\Pi_n\colon L^2(\Omega) \to \mathbb{V}_n$ is the L^2-projection and using V as a test function in (2.3) we obtain the equalities

$$\frac{1}{\tau_n}\|V\|_\Omega^2 + |\!|\!| U_n |\!|\!|_\Omega^2 = \langle f_n,\, V\rangle_\Omega + \mathcal{B}[U_n,\, \Pi_n U_{n-1}] \tag{3.8}$$

and

$$\frac{1}{\tau_n}\|V\|_\Omega^2 + |\!|\!| V |\!|\!|_\Omega^2 = \langle f_n,\, V\rangle_\Omega - \mathcal{B}[\Pi_n U_{n-1},\, V]. \tag{3.9}$$

Using the symmetry of $\mathcal{B}$ and adding (3.8) and (3.9) we compute

$$\frac{2}{\tau_n}\|V\|_\Omega^2 + |\!|\!| V |\!|\!|_\Omega^2 + |\!|\!| U_n |\!|\!|_\Omega^2 = 2\langle f_n,\, V\rangle_\Omega + |\!|\!| \Pi_n U_{n-1} |\!|\!|_\Omega^2.$$

From this we derive by the Cauchy–Schwartz and Young's inequality the bound

$$\frac{1}{\tau_n}\|V\|_\Omega^2 + |\!|\!| V |\!|\!|_\Omega^2 + |\!|\!| U_n |\!|\!|_\Omega^2 \leqslant \tau_n \|f_n\|_\Omega^2 + |\!|\!| \Pi_n U_{n-1} |\!|\!|_\Omega^2.$$

Summing this bound for $n = 1,\dots,m$ in combination with $\sum_{n=1}^m \tau_n\|f_n\|_\Omega^2 \leqslant \|f\|_{\Omega\times(0,t_m)}^2$ proves the claim. □

This uniform energy bound has the following consequence that is a crucial ingredient in the design of our adaptive algorithm in Section 3.3 and in the proof of the main result (Theorem 4.5).

COROLLARY 3.4 (CONTROL OF THE TIME ERROR INDICATOR) If in addition to the assumptions of Proposition 3.6 there holds

$$|\!|\!| U_{n-1} |\!|\!|_\Omega^2 - |\!|\!| \Pi_n U_{n-1} |\!|\!|_\Omega^2 + \frac{1}{\tau_n}\|U_n - \Pi_n U_{n-1}\|_\Omega^2 \geqslant 0 \quad \text{for } n = 1,\dots,N, \tag{3.10}$$

then

$$\sum_{n=1}^{N} |||U_n - \Pi_n U_{n-1}|||_\Omega^2 \leqslant \|f\|_{\Omega\times(0,T)}^2 + |||U_0|||_\Omega^2.$$

In particular, defining for any given $\delta > 0$ the threshold $\tau_* := \delta^2/(\|f\|_{\Omega\times(0,T)}^2 + |||U_0|||_\Omega^2)$, we conclude that

$$\sum_{\substack{n=1\\ \tau_n\leqslant\tau_*}}^{N} \tau_n \mathcal{E}_\tau^2(U_n, U_{n-1}, \tau_n, \mathcal{G}_n) = C_{c\tau} \sum_{\substack{n=1\\ \tau_n\leqslant\tau_*}}^{N} \tau_n |||U_n - \Pi_n U_{n-1}|||_\Omega^2 \leqslant C_{c\tau}\delta^2.$$

This holds true for any sequence of discrete solutions, irrespective of the number of total time steps $N \in \mathbb{N}\cup\{\infty\}$ and the sequence of used time-step sizes $\{\tau_n\}_n^N$.

Proof. Summing the non-negative terms in (3.10) yields

$$0 \leqslant \sum_{n=1}^{m} |||U_{n-1}|||_\Omega^2 - |||\Pi_n U_{n-1}|||_\Omega^2 + \frac{1}{\tau_n}\|U_n - \Pi_n U_{n-1}\|_\Omega^2,$$

which is equivalent to

$$|||U_m|||_\Omega^2 - |||U_0|||_\Omega^2 \leqslant \sum_{n=1}^{m} |||U_n|||_\Omega^2 - |||\Pi_n U_{n-1}|||_\Omega^2 + \frac{1}{\tau_n}\|U_n - \Pi_n U_{n-1}\|_\Omega^2.$$

Adding $\sum_{n=1}^m |||U_n - \Pi_n U_{n-1}|||_\Omega^2$ to both sides and then using Proposition 3.6 results in

$$\sum_{n=1}^{m} |||U_n - \Pi_n U_{n-1}|||_\Omega^2 \leqslant |||U_0|||_\Omega^2 + \|f\|_{\Omega\times(0,t_m)}^2 - |||U_m|||_\Omega^2 \leqslant |||U_0|||_\Omega^2 + \|f\|_{\Omega\times(0,T)}^2,$$

which implies the desired estimate. The final consequence of this bound is then concluded easily from

$$\sum_{\substack{n=1\\ \tau_n\leqslant\tau_*}}^{N} \tau_n |||U_n - \Pi_n U_{n-1}|||_\Omega^2 \leqslant \tau_* \sum_{n=1}^{N} |||U_n - \Pi_n U_{n-1}|||_\Omega^2 \leqslant \tau^*\Big(|||U_0|||_\Omega^2 + \|f\|_{\Omega\times(0,T)}^2\Big),$$

which finishes the proof. □

Assuming that (3.10) holds, the above result gives control of the accumulated time error indicators $\mathcal{E}_\tau^2(U_n, U_{n-1}, \tau_n, \mathcal{G}_n)$ of those time steps with sufficiently small time-step sizes. This means, we can compute *a priori* a threshold τ_* from data f, U_0 and the given tolerance TOL such that the reduction of the time-step size τ_n can be aborted whenever $\tau_n \leqslant \tau_*$ without spoiling the required accuracy of the discrete solution.

The algorithm ASTFEM presented below ensures that (3.10) is fulfilled at the end of any time step, which allows us to use Corollary 3.7 in the analysis of ASTFEM. With this in mind we define the indicators

$$\mathcal{E}_*(v, w, \tau, \mathcal{G}, E) := |||\Pi_{\mathcal{G}} w|||_E^2 - |||w|||_E^2 - \frac{1}{\tau}\|v - \Pi_{\mathcal{G}} w\|_E^2,$$

as well as the convenient notation $\mathcal{E}_*(v, w, \tau, \mathcal{G}) := \sum_{E\in\mathcal{G}} \mathcal{E}_*(v, w, \tau, \mathcal{G}, E)$. Condition (3.10) is then equivalent to $\mathcal{E}_*(U_n, U_{n-1}, \tau_n, \mathcal{G}_n) \leqslant 0$, $n = 1, \ldots, N$.

We would like to remark that (3.10) would be trivially satisfied for the Ritz projection $R_n U_{n-1}$ of U_{n-1} into $\mathbb{V}_n$ since $|\!|\!| R_n U_{n-1} |\!|\!|_\Omega \leqslant |\!|\!| U_{n-1} |\!|\!|_\Omega$. The L^2-projection $\Pi_n U_{n-1}$, however, does not generally provide this monotonicity property. Indeed, using the L^2-projection for U_{n-1} may lead to an increase of energy due to coarsening. This can be observed in experiments. Nevertheless, (3.8) and (3.9) are only valid for the L^2-projection $\Pi_n U_{n-1}$. This is the reason for assuring (3.10) for the accepted solution in our adaptive algorithm. Note that the term $-\frac{1}{\tau}\|v - \Pi_{\mathcal{G}} w\|_E^2$ in (3.10) may compensate for $|\!|\!| \Pi_{\mathcal{G}} w |\!|\!|_E^2 > |\!|\!| w |\!|\!|_E^2$.

3.3 *The adaptive algorithm ASTFEM*

Based on the design principles derived above as well as the gained insights we next describe our adaptive algorithm. To that end we follow a bottom-up approach. We first state the basic properties on some rudimentary modules that are treated as black box modules, then describe two core modules in detail and, finally, collect these procedures in the adaptive algorithm ASTFEM.

3.3.1 *Black box modules.* We use the modules `ADAPT_INIT`, `COARSEN`, `MARK_REFINE` and `SOLVE` as black box routines. In particular, we use the subroutine `MARK_REFINE` in an object-oriented fashion, i.e., the functionality of `MARK_REFINE` changes according to its arguments. We next state the basic properties of these routines.

ASSUMPTION 3.8 (PROPERTIES OF MODULES) We suppose that all rudimentary modules terminate with an output having the following properties:

(1) For a given initial datum u_0 the output

$$(U_0, \mathcal{G}_0) = \texttt{ADAPT\_INIT}(u_0, \mathcal{G}_{\text{init}}, \text{TOL}_0)$$

is a refinement $\mathcal{G}_0 \geqslant \mathcal{G}_{\text{init}}$ and approximation $U_0 \in \mathbb{V}(\mathcal{G}_0)$ to u_0 such that (3.7a) is satisfied, i.e., $\mathcal{E}_0^2(u_0, \mathcal{G}_0) \leqslant \text{TOL}_0^2$.

(2) For given g, $\bar{f}$, τ and $\mathcal{G}$ the output

$$U_\tau = \texttt{SOLVE}(g, \bar{f}, \tau, \mathcal{G})$$

is the solution to the discrete elliptic problem

$$U_\tau \in \mathbb{V}(\mathcal{G}): \quad \frac{1}{\tau}\langle U_\tau, V\rangle_\Omega + \mathcal{B}[U_\tau, V] = \frac{1}{\tau}\langle g, V\rangle_\Omega + \langle \bar{f}, V\rangle_\Omega \text{ for all } V \in \mathbb{V}(\mathcal{G}).$$

Here we assume exact integration and linear algebra.

(3) For given time t, time-step-size τ, grid $\mathcal{G}$, and $U_{\text{old}} \in \mathbb{V}(\mathcal{G})$, the output

$$(\mathcal{G}_-, \tau_+) = \texttt{COARSEN}(f, t, \tau, \mathcal{G}, U_{\text{old}})$$

satisfies $\mathcal{G}_- \leqslant \mathcal{G}$ and $\min\{\tau, T - \tau\} \leqslant \tau_+ \leqslant T - \tau$.

(4) For a given grid $\mathcal{G}$ and a set of indicators $\{\mathcal{E}_E\}_{E\in\mathcal{G}}$ the output

$$\mathcal{G}_+ = \texttt{MARK\_REFINE}(\{\mathcal{E}_E\}_{E\in\mathcal{G}}, \mathcal{G})$$

is a conforming refinement of $\mathcal{G}$, where at least one element in the subset $\arg\max_{E\in\mathcal{G}} \mathcal{E}_E \subset \mathcal{G}$ has been refined.

(5) For given grids $\mathcal{G}, \mathcal{G}_{\text{old}}$ and a set of indicators $\{\mathcal{E}_E\}_{E\in\mathcal{G}}$ the output

$$\mathcal{G}_+ = \texttt{MARK\_REFINE}(\{\mathcal{E}_E\}_{E\in\mathcal{G}}, \mathcal{G}, \mathcal{G}_{\text{old}})$$

is a conforming refinement of $\mathcal{G}$, where at least one element in the set

$$\left\{E \in \mathcal{G} \setminus (\mathcal{G}_{\text{old}} \cap \mathcal{G}) \mid h_{\mathcal{G}|E} > h_{\mathcal{G}_{\text{old}}|E}\right\}$$

has been refined. We call the elements in the above set *coarsened elements in* $\mathcal{G}$ *with respect to* $\mathcal{G}$old.

Some comments on these modules are in order.

REMARK 3.9 (ADAPT_INIT) The task of this module is the (adaptive) approximation of some given function u_0. This is not the subject of the article and therefore ADAPT_INIT is treated as a black box. Density of the finite element spaces in L^2 implies that for any given u_0 there is a grid $\mathcal{G}_0$ and an approximation $U_0 \in \mathbb{V}(\mathcal{G}_0)$ complying with (3.7a).

In the case $d = 2$ and affine finite elements it has been shown that for sufficiently smooth u_0 one can construct an adaptive approximation U_0 with optimal complexity (Binev *et al.*, 2002, Section 5; Nochetto *et al.*, 2009, Section 5).

REMARK 3.10 (SOLVE) The output $U_\tau = \texttt{SOLVE}(g, \bar{f}, \tau, \mathcal{G})$ is the Ritz approximation in $\mathbb{V}(\mathcal{G})$ to the weak solution u_τ of (3.3). Problem (3.3) is a coercive problem with a coercivity constant that does not depend on τ. This implies a uniform inf–sup condition for the discrete spaces. In addition, $\mathcal{E}_\mathcal{G}$ is an estimator for $\|\!|U_\tau - u_\tau|\!\|_\Omega$, where the constant of the upper bound is independent of τ, but the constant of the lower bound depends on τ.

It is important for the discussion below that these properties imply for a fixed τ the assumptions on the modules SOLVE and ESTIMATE of the basic convergence results for adaptive finite elements in Morin *et al.* (2008) and Siebert (2011); compare with Proposition 4.2 below.

REMARK 3.11 (COARSEN) We apply COARSEN$(f, t, \tau, \mathcal{G}, U_{\text{old}})$ at the beginning of each time-step with time $t = t_{n-1}$, time-step-size $\tau = \tau_{n-1}$, grid $\mathcal{G} = \mathcal{G}_{n-1}$ and the solution $U_{\text{old}} = U_{n-1}$ from the previous time-step so as to remove degrees of freedom and to enlarge the time-step-size. Starting with this coarser mesh $\mathcal{G}_-$ and enlarged time-step-size τ_+ we then allow in a second phase only for mesh refinement and time-step-size reduction in order to compute a discrete solution with sufficient accuracy.

Basically, COARSEN $(f, t, \tau, \mathcal{G}, U_{\text{old}})$ may ignore the argument f when enlarging τ by returning any value in the range $\tau \leqslant \tau_+ \leqslant T - t$. But for the sake of efficiency it is more appropriate that the enlarged time-step-size τ_+ is chosen such that the consistency error is below or, at least, close to tolerance, this means $\mathcal{E}_f^2(f, t, \tau_+) \leqslant \text{TOL}_f^2$ or $\mathcal{E}_f^2(f, t, \tau_+) \approx \text{TOL}_f^2$.

Similarly, it is not necessary that the coarsening error $\mathcal{E}_c^2(U_{\text{old}}, \mathcal{G}) = C_{c\tau}\|\!|\Pi_\mathcal{G} U_{\text{old}} - U_{\text{old}}|\!\|_\Omega^2$ is controlled by COARSEN. This means, COARSEN$(f, t, \tau, \mathcal{G}, U_{\text{old}})$ may ignore the argument U_{old} by returning any grid that is coarser than $\mathcal{G}$; in the extreme case this could be $\mathcal{G}_{\text{init}}$. Recalling the upper

bound in Theorem 3.1 we realize that the accuracy of the discrete solution is particularly influenced by the coarsening error $\mathcal{E}_c$; compare also with (3.2). Consequently, the adaptive procedure in the second phase has to take care of $\mathcal{E}_c$. In view of this, and bearing in mind Remark (3.4), a better choice is some grid $\mathcal{G}_-$ such that U_{old} is still approximated well in $\mathbb{V}(\mathcal{G}_-)$, for instance $\|\!|I_- U_{\text{old}} - U_{\text{old}}|\!\|_\Omega$ is "small" for some projection or interpolation operator $I_- : V \to \mathbb{V}(\mathcal{G}_-)$.

A consistency error close to tolerance and a sufficiently small coarsening error typically reduce the number of adaptive iterations in the second phase and thereby the computational cost. In the numerical experiments in Section 5.3 we try to double the actual time-step-size if the consistency error is sufficiently small: if $\mathcal{E}_f^2(f,t,\tau) < \frac{1}{2}\text{TOL}_f^2$ we return $\tau_+ = \min\{2\tau, T-t\}$ and else we return $\tau_+ = \tau$. Moreover, we use information about U_{n-1} when constructing $\mathcal{G}_-$; some details on mesh coarsening are given in Section 5.2.

REMARK 3.12 (MARK_REFINE I) We apply MARK_REFINE($\{\mathcal{E}_E\}_{E\in\mathcal{G}}, \mathcal{G}$) with the estimator $\mathcal{E}_\mathcal{G}$ for the elliptic problem (3.3). The typical realization of such a routine is a two-step procedure. Initially, a subset $\mathcal{M} \subset \mathcal{G}$ of marked elements is selected using the information of the indicators $\{\mathcal{E}_E\}_{E\in\mathcal{G}}$. Hereby, well-known marking strategies like the maximum strategy, equidistribution strategy or (nearly) minimal Dörfler marking can be used. In a second step all marked elements are refined with REFINE($\mathcal{M}, \mathcal{G}$) producing a conforming refinement $\mathcal{G}_+$.

This procedure entails Assumption 3.8 (4), which itself implies the property of marking used in the basic convergence results for adaptive finite elements in Morin *et al.* (2008) and Siebert (2011).

REMARK 3.13 (MARK_REFINE II) We apply MARK_REFINE($\{\mathcal{E}_E\}_{E\in\mathcal{G}}, \mathcal{G}, \mathcal{G}_{\text{old}}$) with the coarsening indicator $\mathcal{E}_c$ and the indicator $\mathcal{E}_*$ controlling the gain of energy. Whenever $\mathcal{G}$ is a refinement of $\mathcal{G}_{\text{old}}$ the coarsening indicator vanishes and condition (3.10) is ensured, i.e., $\mathcal{E}_c = 0$ and $\mathcal{E}_* \leqslant 0$ for $\mathcal{G}_{\text{old}} \leqslant \mathcal{G}$. In view of this, it is reasonable to only refine coarsened elements. Consequently, Assumption 3.8 (5) is minimal.

Nevertheless, for efficiency reasons this can be tuned by using information supplied by the indicators $\{\mathcal{E}_E\}_{E\in\mathcal{G}}$, for instance, selecting those coarsened elements with large indicators. Assumption 3.8 (5) entails that recurrent application of MARK_REFINE($\{\mathcal{E}_E\}_{E\in\mathcal{G}}, \mathcal{G}, \mathcal{G}_{\text{old}}$) with the same $\mathcal{G}_{\text{old}}$ results in a grid $\mathcal{G}_+$ with $\mathcal{G}_{\text{old}} \leqslant \mathcal{G}_+$ within finitely many iterations and consequently $\mathcal{E}_c = \mathcal{E}_* = 0$.

3.3.2 *The core modules.* We start with the module CONSISTENCY, listed in Algorithm 1, controlling the consistency error $\mathcal{E}_f$, which is below the given tolerance upon termination. Recalling its definition in (3.1b) we see that the consistency error is solely influenced by the right-hand side f, time t and the time-step-size τ, but not by the discrete solution. CONSISTENCY is executed at the beginning of each time-step to give an initial guess for the time-step-size and after each further reduction of the time-step-size. The latter is necessary to control a possible increase of the consistency error, which is in general not monotone with respect to the time-step-size. We shall show below in Lemma 4.1 that CONSISTENCY does not reduce τ below a threshold $\tau_f > 0$ that can be computed from regularity properties of f. Note that CONSISTENCY can be entered with $\tau \leqslant \tau_f$.

We next turn to the module ST_ADAPTATION, listed in Algorithm 2, which adapts the grid and time-step-size according to the consistency indicator $\mathcal{E}_f$, space indicator $\mathcal{E}_\mathcal{G}$ and time-coarsening indicator $\mathcal{E}_{c\tau}$, respectively, the separated coarsening indicator $\mathcal{E}_c$ and time indicator $\mathcal{E}_\tau$. As stated above, any reduction of the time-step-size τ due to $\mathcal{E}_\tau$ requires an additional execution of CONSISTENCY to ensure that $\mathcal{E}_f^2(f,t,\tau) \leqslant \text{TOL}_f^2$.

The main part of the module is a loop that requires right at the start the computation of the discrete solution on the actual grid and with the current time-step-size. Basically, it is a typical adaptive

Algorithm 1 Module `CONSISTENCY` (Parameters $\delta \in (0,1)$)

`CONSISTENCY`$(f, t, \tau, \mathrm{TOL}_f)$

1: compute $\mathcal{E}_f^2(f,t,\tau)$
2: **while** $\mathcal{E}_f^2(f,t,\tau) > \mathrm{TOL}_f^2$ **do** ★ reduce τ
3: $\quad \tau = \delta\tau$
4: $\quad$ compute $\mathcal{E}_f^2(f,t,\tau)$
5: **end while**
6: $\bar{f} = \fint_t^{t+\tau} f(s)\,ds$
7: **return** $\bar{f}, \tau$

iteration for an adaptive time-stepping scheme subject to the following restrictions. Firstly, adaptation in space is restricted to refinement. Secondly, the time-step-size is only reduced but not below $\min\{\tau_*, \tau_f\}$, where the threshold $\tau_* > 0$ is provided as an argument by the superordinated routine ASTFEM. The module can, however, be entered with a time-step-size $\tau < \min\{\tau_*, \tau_f\}$. We next turn to the module `ST_ADAPTATION`, listed in Algorithm 2, which adapts the grid and time-step size according to the space indicator $\mathcal{E}_\mathcal{G}$ and time–coarsening indicator $\mathcal{E}_{c\tau}$, respectively, the separated coarsening indicator $\mathcal{E}_c$ and time indicator $\mathcal{E}_\tau$. The routine is an iteration that requires right at the start the computation of the discrete solution on the actual grid and with the current time-step size.

Basically, it is a typical adaptive iteration for an adaptive time-stepping scheme subject to the following restrictions. Firstly, adaptation in space is restricted to refinement. Secondly, the time-step size is only reduced but never below a given threshold $\tau_* > 0$, which is provided by the superordinated routine ASTFEM. Note, however, that the module can be entered with a time-step size $\tau < \tau_*$. Finally, the appropriate action to be taken is selected adaptively; that is, rather than processing certain adaptive actions in a fixed order, we compare the relative sizes of the various indicators to determine which adaptive action is currently most appropriate. This approach complicates the presentation; however, it leads to a more adaptive algorithm since it always addresses the dominating indicator. Ultimately, this results in an improved performance; compare with Section 5.3.

The adaptive iteration can only be abandoned at two instances; the first one in line 6 and the second one in line 19 of Algorithm 2. In the first case the sum of the spatial and time–coarsening indicators is below tolerance, i.e.,

$$\mathcal{E}_\mathcal{G}^2(U, U_{\mathrm{old}}, \tau, \bar{f}, \mathcal{G}) + \mathcal{E}_{c\tau}^2(U, U_{\mathrm{old}}, \mathcal{G}) \leqslant \mathrm{TOL}_{\mathcal{G}\tau}^2, \tag{3.11a}$$

and this we denote as *standard exit*. In the latter case the algorithm only controls the space and coarsening indicators. Leaving through this *nonstandard exit* with $\tau \leqslant \tau_*$ there holds

$$\mathcal{E}_\mathcal{G}^2(U, U_{\mathrm{old}}, \tau, \bar{f}, \mathcal{G}) + 2\mathcal{E}_c^2(U_{\mathrm{old}}, \mathcal{G}) \leqslant \mathrm{TOL}_{\mathcal{G}\tau}^2. \tag{3.11b}$$

The uncontrolled indicator $\mathcal{E}_\tau$ is implicitly handled at this place with an appropriate choice of the threshold τ_* by ASTFEM in combination with Corollary 3.7.

3.3.3 *The main module ASTFEM.* We are now in a position to formulate the overall algorithm ASTFEM, which is listed in Algorithm 3. In the initialization phase the given tolerance $\mathrm{TOL} > 0$ is split into

Algorithm 2 Module ST_ADAPTATION (Parameter $\delta \in (0, 1)$)

ST_ADAPTATION$(U_{\text{old}}, f, t, \tau, \mathcal{G}, \mathcal{G}_{\text{old}}, \tau_*, \text{TOL}_{\mathcal{G}\tau}, \text{TOL}_f)$

1: $(\bar{f}, \tau) =$ CONSISTENCY$(f, t, \tau, \text{TOL}_f)$
2: **loop forever**
3: $U =$ SOLVE$(U_{\text{old}}, \bar{f}, \tau, \mathcal{G})$
4: compute $\{\mathcal{E}^2_{\mathcal{G}}(U, U_{\text{old}}, \tau, \bar{f}, \mathcal{G}, E)\}_{E\in\mathcal{G}}$ and $\mathcal{E}^2_{c\tau}(U, U_{\text{old}}, \mathcal{G})$
5: **if** $\mathcal{E}^2_{\mathcal{G}}(U, U_{\text{old}}, \tau, \bar{f}, \mathcal{G}) + \mathcal{E}^2_{c\tau}(U, U_{\text{old}}, \mathcal{G}) \leqslant \text{TOL}^2_{\mathcal{G}\tau}$ **then**
6: **break** ★ std. exit
7: **else if** $\mathcal{E}^2_{\mathcal{G}}(U, U_{\text{old}}, \tau, \bar{f}, \mathcal{G}) > \mathcal{E}^2_{c\tau}(U, U_{\text{old}}, \mathcal{G})$ **then** ★ $\mathcal{E}_{\mathcal{G}}$ dominates
8: $\mathcal{G} =$ MARK_REFINE$(\{\mathcal{E}^2_{\mathcal{G}}(U, U_{\text{old}}, \tau, \bar{f}, \mathcal{G}, E)\}_{E\in\mathcal{G}}, \mathcal{G})$ A
9: **else** ★ $\mathcal{E}_{c\tau}$ dominates
10: compute $\mathcal{E}^2_{\tau}(U, U_{\text{old}}, \mathcal{G})$ and $\{\mathcal{E}^2_c(U_{\text{old}}, \mathcal{G}, E)\}_{E\in\mathcal{G}}$
11: **if** $\tau > \tau_*$ **then**
12: **if** $\mathcal{E}^2_{\tau}(U, U_{\text{old}}, \mathcal{G}) > \mathcal{E}^2_c(U_{\text{old}}, \mathcal{G})$ **then** ★ $\mathcal{E}_{\tau}$ dominates
13: $\tau = \max\{\delta\tau, \tau_*\}$ B
14: $(\bar{f}, \tau) =$ CONSISTENCY$(f, t, \tau, \text{TOL}_f)$
15: **else** ★ $\mathcal{E}_c$ dominates
16: $\mathcal{G} =$ MARK_REFINE$(\{\mathcal{E}^2_c(U_{\text{old}}, \mathcal{G}, E)\}_{E\in\mathcal{G}}, \mathcal{G}, \mathcal{G}_{\text{old}})$ C
17: **end if**
18: **else if** $\mathcal{E}^2_{\mathcal{G}}(U, U_{\text{old}}, \tau, \bar{f}, \mathcal{G}) + 2\mathcal{E}^2_c(U_{\text{old}}, \mathcal{G}) \leqslant \text{TOL}^2_{\mathcal{G}\tau}$ **then**
19: **break** ★ non-std. exit
20: **else**
21: **if** $\mathcal{E}^2_{\mathcal{G}}(U, U_{\text{old}}, \tau, \bar{f}, \mathcal{G}) > 2\mathcal{E}^2_c(U_{\text{old}}, \mathcal{G})$ **then** ★ $\mathcal{E}_{\mathcal{G}}$ dominates
22: $\mathcal{G} =$ MARK_REFINE$(\{\mathcal{E}^2_{\mathcal{G}}(U, U_{\text{old}}, \tau, \bar{f}, \mathcal{G}, E)\}_{E\in\mathcal{G}}, \mathcal{G})$ D
23: **else** ★ $\mathcal{E}_c$ dominates
24: $\mathcal{G} =$ MARK_REFINE$(\{\mathcal{E}^2_c(U_{\text{old}}, \mathcal{G}, E)\}_{E\in\mathcal{G}}, \mathcal{G}, \mathcal{G}_{\text{old}})$ E
25: **end if**
26: **end if**
27: **end if**
28: **end loop forever**
29: **return** $U, \tau, \bar{f}, \mathcal{G}$

$$\mathrm{TOL}_0^2 + T\,\mathrm{TOL}_f^2 + T\,\mathrm{TOL}_{\mathcal{G}\tau}^2 + \mathrm{TOL}_*^2 = \mathrm{TOL}^2 \tag{3.12}$$

with $\mathrm{TOL}_0, \mathrm{TOL}_f, \mathrm{TOL}_{\mathcal{G}\tau}, \mathrm{TOL}_* > 0$. The additional tolerance TOL_* will be used for bounding the uncontrolled indicators $\mathcal{E}_\tau$ of the nonstandard exit in ST_ADAPTATION. It may be chosen much smaller than the other tolerances. Next ADAPT_INIT provides a sufficiently good approximation U_0 of the initial datum u_0, and we finalize this phase by computing the threshold

$$\tau_* := \frac{\mathrm{TOL}_*^2}{2C_{c\tau}(\|f\|_{\Omega\times(0,T)}^2 + |||U_0|||_\Omega^2)}, \tag{3.13}$$

which serves as *minimal time-step size* for ST_ADAPTATION.

We then enter the time-step iteration, where each single time-step consists of the following main steps. We first initialize the time-step size and grid by one coarsening step with COARSEN.

The adaptation of the grid and time-step size with respect to the indicators for the spatial, temporal and coarsening error is done by ST_ADAPTATION, which returns a new solution U_n. If the current pair (U_n, U_{n-1}) complies with condition (3.10) for the uniform energy estimate, U_n is accepted as the final solution of the time step. Otherwise, an increase in energy has to be reduced by appropriate refinements.

After modifying the mesh in order to reduce an increase in energy, the indicators $\mathcal{E}_\mathcal{G}$, $\mathcal{E}_{c\tau}$, respectively, $\mathcal{E}_\mathcal{G}$, $\mathcal{E}_c$, may not be below the tolerance, i.e., (3.11) is not met. Moreover, the output of a rerun of ST_ADAPTATION may again violate (3.10). Consequently, these two steps have to be iterated.

Algorithm 3 ASTFEM

initialize $\mathcal{G}_{\text{init}}$, τ_0 and set $t_0 = 0$, $n = 0$
split tolerance $\mathrm{TOL} > 0$ such that $\mathrm{TOL}_0^2 + T\,\mathrm{TOL}_f^2 + T\,\mathrm{TOL}_{\mathcal{G}\tau}^2 + \mathrm{TOL}_*^2 = \mathrm{TOL}^2$
$(U_0, \mathcal{G}_0) = \mathtt{ADAPT\_INIT}(u_0, \mathcal{G}_{\text{init}}, \mathrm{TOL}_0)$
compute threshold τ_* by (3.13) from $(U_0, f, \mathrm{TOL}_*^2)$
do
    $n = n + 1$
    $\tau_n = \min\{\tau_{n-1}, T - t_{n-1}\}$
    $(\mathcal{G}_n, \tau_n) = \mathtt{COARSEN}(f, t_{n-1}, \tau_{n-1}, \mathcal{G}_{n-1}, U_{n-1})$
    loop forever
        $(U_n, \tau_n, f_n, \mathcal{G}_n) = \mathtt{ST\_ADAPTATION}(U_{n-1}, f, t_{n-1}, \tau_n, \mathcal{G}_n, \mathcal{G}_{n-1}, \tau_*, \mathrm{TOL}_{\mathcal{G}\tau}, \mathrm{TOL}_f)$
        compute $\{\mathcal{E}_*(U_n, U_{n-1}, \tau_n, \mathcal{G}_n, E)\}_{E\in\mathcal{G}_n}$
        if $\mathcal{E}_*(U_n, U_{n-1}, \tau_n, \mathcal{G}_n) > 0$ **then** ★ control energy gain
            $\mathcal{G}_n = \mathtt{MARK\_REFINE}(\{\mathcal{E}_*(U_n, U_{n-1}, \tau_n, \mathcal{G}_n, E)\}_{E\in\mathcal{G}_n}, \mathcal{G}_n, \mathcal{G}_{n-1})$
        else
            break ★ accept time-step
        end if
    end loop forever
while $t_n = t_{n-1} + \tau_n < T$

4. Convergence analysis for ASTFEM

In this section we first prove that the core modules and ASTFEM terminate and then verify that the space–time error is below the given tolerance. Throughout this section we suppose that the black box modules satisfy Assumption 3.8

We start with termination of the module CONSISTENCY.

LEMMA 4.1 (TERMINATION OF CONSISTENCY) Assume $f \in H^1((0,T); L^2(\Omega))$ and set

$$\tau_f := \frac{\delta \mathrm{TOL}_f^2}{C_f \|\partial_t f\|^2_{\Omega\times(0,T)}}. \tag{4.1}$$

Then for any $t \in (0,T)$ and $\tau_{\mathrm{in}} \in (0, T-t]$,

$$(\bar f, \tau) = \mathtt{CONSISTENCY}(f, t, \tau_{\mathrm{in}}, \mathrm{TOL}_f)$$

terminates with

$$\tau_{in} \geqslant \tau \geqslant \min\{\tau_f, \tau_{\mathrm{in}}\} \quad \text{and} \quad \mathcal{E}_f^2(f,t,\tau) \leqslant \mathrm{TOL}_f^2.$$

Proof. Lemma 3.2 in combination with the definition of τ_f yields

$$\mathcal{E}_f^2(f,t,\tau) \leqslant \mathrm{TOL}_f^2 \quad \text{for all } \tau \leqslant \tau_f/\delta. \tag{4.2}$$

In each iteration of the **while** loop the time-step size τ is reduced by a constant factor δ and we enter this loop with $\tau_f/\delta_1 \leqslant \tau \leqslant T-t$. Consequently, (4.2) implies that this loop is iterated only a finite number of times and the smallest time-step size τ that might be produced is bounded from below by τ_f. This proves the assertion. □

Before turning to the main module ST_ADAPTATION we need the following result for the elliptic problem (3.3).

PROPOSITION 4.2 (CONVERGENCE FOR THE ELLIPTIC PROBLEM) Suppose that $g, \bar f \in L^2(\Omega)$ and $\tau > 0$ are fixed data for the elliptic problem (3.3) and let $u_\tau \in \mathbb{V}$ be its weak solution. Starting from any grid $\mathcal{G}^0 \in \mathbb{G}$ we denote by $\{\mathcal{G}^k, U_\tau^k\}_{k\geqslant 0}$ the sequence of grids and corresponding Ritz approximations in $\mathbb{V}(\mathcal{G}^k)$ to u_τ, which are computed adaptively by recurrent application of the modules SOLVE and MARK_REFINE utilizing the spatial estimator $\mathcal{E}_{\mathcal{G}}$.

Then there exists a $K > 0$ such that

$$\mathcal{E}_{\mathcal{G}}^2\big(U_\tau^K, g, \tau, \bar f, \mathcal{G}^K\big) \leqslant \frac{1}{2}\mathrm{TOL}_{\mathcal{G}_\tau}^2.$$

Proof. Properties of the elliptic problem, SOLVE, the estimator $\mathcal{E}_{\mathcal{G}}$ and MARK_REFINE, which utilizes refinement by bisection of simplicial grids, imply the assumptions of the basic convergence results for adaptive finite elements in Morin *et al.* (2008) and Siebert (2011); compare also with Remarks 3.10 and 3.12 Applying the main results of Morin *et al.* (2008) and Siebert (2011) then yields the proposition. □

This brings us into position to show termination of ST_ADAPTATION.

LEMMA 4.3 (TERMINATION OF ST_ADAPTATION) For any $t \in (0,T)$, $\tau_{\mathrm{in}} \in (0, T-t]$, $\mathcal{G}, \mathcal{G}_{\mathrm{old}} \in \mathbb{G}$ and $U_{\mathrm{old}} \in \mathbb{V}(\mathcal{G}_{\mathrm{old}})$,

$$(U, \tau, \bar f, \mathcal{G}) = \mathtt{ST\_ADAPTATION}(U_{\mathrm{old}}, f, t, \tau_{\mathrm{in}}, \mathcal{G}_{\mathrm{in}}, \mathcal{G}_{\mathrm{old}}, \tau_*, \mathrm{TOL}_{\mathcal{G}_\tau}, \mathrm{TOL}_f)$$

terminates with a time-step-size τ satisfying

$$\tau_{\text{in}} \geqslant \tau \geqslant \min\{\tau_{\text{in}}, \tau_*, \tau_f\},$$

$\mathcal{E}_f^2(f, t, \tau) \leqslant \text{TOL}_f^2$, and a discrete solution $U \in \mathbb{V}(\mathcal{G})$ on a refinement $\mathcal{G} \leqslant \mathcal{G}_{\text{in}}$ that fulfils (3.11a) or (3.11b). In the latter case one has $\tau \leqslant \tau_*$.

Proof. In Lemma 4.1 we have shown that CONSISTENCY terminates with $\mathcal{E}_f^2(f, t, \tau) \leqslant \text{TOL}_f^2$ and a time-step-size that is not enlarged and not below τ_f . This particularly implies that ST-ADAPTATION only reduces the time-step-size, which shows $\tau_{\text{in}} \geqslant \tau$. The module CONSISTENCY is executed at the beginning and in case B, which are the only places, where the time-step-size is reduced. In B the time-step-size τ is initially reduced, but not below τ_*. The subsequent execution of CONSISTENCY, controlling a possible increase of the consistency error, may further reduce τ but not below τ_f. Summarizing, whenever ST-ADAPTATION terminates there holds $\tau \geqslant \min\{\tau_{\text{in}}, \tau_*, \tau_f\}$ and $\mathcal{E}_f^2(f, t, \tau) \leqslant \text{TOL}_f^2$.

It remains to show termination of ST-ADAPTATION. In each run of the iteration either the time-step-size is reduced or the actual grid is refined. More precisely, exactly one of the statements labeled as A,. . . ,E in Algorithm 2 is executed, any of them terminating by Assumption 3.6 and Lemma 4.1. Whenever one of these statements is executed the corresponding indicator is positive.

In statement B the time-step-size is reduced by a constant factor $\delta < 1$. This is only done if $\tau > \tau_*$, which therefore can only happen finitely many times.

In statements C and E the grid is refined due to the coarsening indicator $\mathcal{E}_c$. Since we are only using refinement, Assumption 3.8 (5) implies that a finite number of executions of C and E results in a grid $\mathcal{G}$ with $\mathcal{G}_{\text{old}} \leqslant \mathcal{G}$; compare with Remark 3.13. This happens irrespective of other refinements in statements A and D. In this situation one has $\mathcal{E}_c^2(U_{\text{old}}, \mathcal{G}) = 0$ and we conclude that these statements can only be carried out finitely many times.

Assuming that ST_ADAPTATION does not terminate, we therefore infer that statements A or D have to be executed infinitely many times. Whenever these statements are performed one has $\mathcal{E}_{\mathcal{G}}^2(U, U_{\text{old}}, \tau, \bar{f}, \mathcal{G}) > \frac{1}{2}\text{TOL}_{\mathcal{G}\tau}^2$. This follows from the if conditions on lines 5 and 7, respectively, the if conditions on lines 18 and 21.

Since all other statements are only conducted finitely many times, there is an iteration count after that only the statements A and D are executed. After this point the time-step size is not reduced and the loop reduces to an adaptive iteration for the elliptic problem (3.3) with fixed data U_{old}, $\bar{f}$ and τ complying with the assumptions of Proposition 4.2. Therefore, after a limited number of iterations we obtain a discrete solution U with $\mathcal{E}_{\mathcal{G}}^2(U, U_{\text{old}}, \tau, \bar{f}, \mathcal{G}) \leqslant \frac{1}{2}\text{TOL}_{\mathcal{G}\tau}^2$, a contradiction.

In summary, we deduce that ST_ADAPTATION terminates and the iteration is abandoned at line 6 or 19, which implies the claim about the time-step size and the size of the indicators. □

We next address termination of the main module ASTFEM.

PROPOSITION 4.4 (TERMINATION OF ASTFEM) The adaptive algorithm ASTFEM terminates for any initial time-step size $\tau_0 > 0$ and produces a finite number of time instances $0 = t_0 < \cdots < t_N = T$, where the produced time-step sizes fulfil

$$\tau_n \geqslant \min\{\tau_f, \tau_*, \tau_0\}, \quad n = 1, \ldots, N-1 \quad \text{and} \quad \tau_N = T - t_{N-1}.$$

The initial error satisfies (3.7a). At the end of any time step the consistency error complies with (3.7b), the indicators for the spatial, coarsening and time error evaluated in the accepted solutions U_n meet (3.11) and the indicator controlling an increase in energy is nonpositive, i.e., (3.10) holds.

Proof. Each loop starts with setting the time-step size such that $\tau_n \leqslant T - t_n$, where $n \in \mathbb{N}$. All modules of ASTFEM terminate. This follows from Assumption 3.8 for the black box modules and Lemma 4.3 for ST_ADAPTATION. Therefore, we only have to consider termination of the loop on lines 9–17 in Algorithm 3. This we conclude from Assumption 3.8 (5) as follows.

Recalling Remark 3.13, recurrent control of an increase in energy in line 13, i.e., recurrent application of $\texttt{MARK\_REFINE}(\{\mathcal{E}_*(U_n, U_{n-1}, \tau_n, \mathcal{G}_n, E)\}_{E\in\mathcal{G}_n}, \mathcal{G}_n, \mathcal{G}_{n-1})$, produces within finitely many iterations a grid $\mathcal{G}_n$ such that $\mathcal{G}_{n-1} \leqslant \mathcal{G}_n$. This happens irrespective of any further refinements in ST_ADAPTATION. By definition of the indicator $\mathcal{E}_*$ this implies $\mathcal{E}_*(U_n, U_{n-1}, \tau_n, \mathcal{G}_n) \leqslant 0$, whence the loop is abandoned and the time-step is accepted.

As long as $\tau_n < T - t_n$ remains valid, we conclude from Lemmas 4.1 and 4.3 that

$$\tau_n \geqslant \min\{\tau_f, \tau_*, \tau_0\} > 0.$$

This implies that final time T is reached with a finite number N of time steps as well as the claim about the time-step sizes.

The claim for the indicators follows from Assumption 3.8 (1), Lemma 4.3, and termination of the loop in ASTFEM. □

Collecting the results derived above allows us to prove the main result of this article.

THEOREM 4.5 (CONVERGENCE INTO TOLERANCE) Let $\mathcal{L}$ be an elliptic differential operator complying with the assumptions stated in Section 2.1, $f \in H^1((0,T); L^2(\Omega))$ and $u_0 \in L^2(\Omega)$ be data to (2.2) and let $u \in \mathbb{W}(0,T)$ be the weak solution.

Algorithm ASTFEM computes for any given tolerance $\mathrm{TOL} > 0$ and initial time-step size $\tau_0 > 0$ an approximation $U \in \mathbb{W}(0,T)$ from discrete values $U_n \in \mathbb{V}(\mathcal{G}_n)$ given by (2.3) over a suitable partition $0 < t_0 < \cdots < t_N = T$ with corresponding adaptive meshes $\{\mathcal{G}_n\}_{n=0,\dots,N}$ such that

$$\|u - U\|_{\mathbb{W}(0,T)} \leqslant \mathrm{TOL}.$$

Proof. Termination of the algorithm has been shown in Proposition 4.4, whence it remains to prove the error bound.

The initial error satisfies $\mathcal{E}_0^2(u_0, \mathcal{G}_0) \leqslant \mathrm{TOL}_0^2$ by assumption. The consistency error satisfies at the end of any time step (3.7b), which gives

$$\sum_{n=1}^{N} \tau_n \mathcal{E}_f^2(f, t_{n-1}, \tau_n) \leqslant \sum_{n=1}^{N} \tau_n \,\mathrm{TOL}_f^2 = T\,\mathrm{TOL}_f^2.$$

When finalizing a time step we also have (3.11), this is

$$\mathcal{E}_{\mathcal{G}}^2(U_n, U_{n-1}, \tau_n, f_n, \mathcal{G}_n) + \mathcal{E}_{c\tau}^2(U_n, U_{n-1}, \mathcal{G}_n) \leqslant \mathrm{TOL}_{\mathcal{G}_\tau}^2 \tag{4.3a}$$

or

$$\mathcal{E}_{\mathcal{G}}^2(U_n, U_{n-1}, \tau_n, f_n, \mathcal{G}_n) + 2\mathcal{E}_{c}^2(U_{n-1}, \mathcal{G}_n) \leqslant \mathrm{TOL}_{\mathcal{G}_\tau}^2, \tag{4.3b}$$

where in the latter case $\tau_n \leqslant \tau_*$.

Summing over those time-steps with $\tau_n > \tau_*$ we deduce from (4.3a)

$$\sum_{\substack{n=1\\ \tau_n>\tau_*}}^{N} \tau_n \Big(\mathcal{E}_{\mathcal{G}}^2(U_n, U_{n-1}, \tau_n, f_n, \mathcal{G}_n) + \mathcal{E}_{c\tau}^2(U_n, U_{n-1}, \mathcal{G}_n)\Big) \leqslant \mathrm{TOL}_{\mathcal{G}_\tau}^2 \sum_{\substack{n=1\\ \tau_n>\tau_*}}^{N} \tau_n. \tag{4.4}$$

We next turn to the case $\tau_n \leqslant \tau_*$. We observe that $\mathcal{E}_*(U_n, U_{n-1}, \tau_n, \mathcal{G}_n) \leqslant 0$ holds at the end of all time steps. Consequently, we can apply Corollary 3.7 with $\tau_* = \mathrm{TOL}_*^2/(2C_{c\tau}(\|f\|^2_{\Omega\times(0,T)} + |\!|\!|U_0|\!|\!|^2_\Omega))$ from (3.13) to obtain

$$2\sum_{\substack{n=1\\ \tau_n\leqslant\tau_*}}^{N} \tau_n \mathcal{E}_\tau^2(U_n, U_{n-1}, \mathcal{G}_n) \leqslant \mathrm{TOL}_*^2. \tag{4.5}$$

Splitting the coarsening–time indicator $\mathcal{E}_{c\tau}$ into $\mathcal{E}_c$ and $\mathcal{E}_\tau$ we deduce from (4.3b) that

$$\begin{aligned}
&\tau_n \mathcal{E}_{\mathcal{G}}^2(U_n, U_{n-1}, \tau_n, f_n, \mathcal{G}_n) + \tau_n \mathcal{E}_{c\tau}^2(U_n, U_{n-1}, \mathcal{G}_n)\\
&\quad\leqslant \tau_n \mathcal{E}_{\mathcal{G}}^2(U_n, U_{n-1}, \tau_n, f_n, \mathcal{G}_n) + 2\tau_n \mathcal{E}_c^2(U_{n-1}, \mathcal{G}_n) + 2\tau_n \mathcal{E}_\tau^2(U_n, U_{n-1}, \mathcal{G}_n)\\
&\quad\leqslant \tau_n\, \mathrm{TOL}_{\mathcal{G}_\tau}^2 + 2\tau_n \mathcal{E}_\tau^2(U_n, U_{n-1}, \mathcal{G}_n).
\end{aligned}$$

Summing over the time steps with $\tau_n \leqslant \tau_*$ and using (4.5) gives

$$\sum_{\substack{n=1\\ \tau_n\leqslant\tau_*}}^{N} \tau_n \Big(\mathcal{E}_{\mathcal{G}}^2(U_n, U_{n-1}, \tau_n, f_n, \mathcal{G}_n) + \mathcal{E}_{c\tau}^2(U_n, U_{n-1}, \mathcal{G}_n)\Big) \leqslant \mathrm{TOL}_{\mathcal{G}_\tau}^2 \sum_{\substack{n=1\\ \tau_n\leqslant\tau_*}}^{N} \tau_n + \mathrm{TOL}_*^2. \tag{4.6}$$

Finally, we collect the results of the two cases by adding (4.4) and (4.6) to deduce that

$$\sum_{n=1}^{N} \tau_n \Big(\mathcal{E}_{\mathcal{G}}^2(U_n, U_{n-1}, \tau_n, f_n, \mathcal{G}_n) + \mathcal{E}_{c\tau}^2(U_n, U_{n-1}, \mathcal{G}_n)\Big) \leqslant T\,\mathrm{TOL}_{\mathcal{G}_\tau}^2 + \mathrm{TOL}_*^2.$$

Collecting the bounds for the indicators $\mathcal{E}_0$, $\mathcal{E}_{\mathcal{G}}$, $\mathcal{E}_{c\tau}$ and $\mathcal{E}_f$, recalling the splitting (3.12) of the tolerance

$$\mathrm{TOL}_0^2 + T\,\mathrm{TOL}_f^2 + T\,\mathrm{TOL}_{\mathcal{G}_\tau}^2 + \mathrm{TOL}_*^2 = \mathrm{TOL}^2,$$

and taking into account the upper bound of Theorem 3.1 we have proven $\|U - u\|_{\mathbb{W}(0,T)} \leqslant \mathrm{TOL}$. □

5. Numerical aspects and experiments

We conclude this article by describing some practical aspects of the implementation and with two numerical experiments. In each experiment we compare our algorithm with a variant of the Chen and Feng algorithm.

5.1 *Aspects of the implementation*

The algorithm was implemented using the adaptive finite element toolbox ALBERTA (Schmidt & Siebert, 2005; Schmidt *et al.*, 2005), which provides piecewise polynomial Lagrange elements over simplicial meshes and bisection for local refinement. The results shown below utilize piecewise affine finite elements in space.

Due to spatial adaptivity in each time step, we need to handle two different meshes and corresponding finite element functions at the same time—the old solution $U_{n-1} \in \mathbb{V}_{n-1}$ on the old mesh $\mathcal{G}_{n-1}$ and the new solution $U_n \in \mathbb{V}_n$ on a typically locally coarsened and refined new mesh $\mathcal{G}_n$. Taking advantage of the hierarchical structure of meshes, which are refined locally differently but originate from the same macro triangulation, it is possible to implement grid transfers to locally finer or coarser mesh elements

very efficiently. Meshes refined by bisection correspond to a collection of binary trees, one for each macro element, where each parent element owns two children elements, produced by refining the parent by bisection. A combined traversal of two different trees (of the same macro element) corresponding to different local refinements (in $\mathcal{G}_{n-1}$ and $\mathcal{G}_n$) can be exploited to evaluate finite element functions on interpolation or quadrature points of a subgrid, see (Schmidt, 2003a,b) for details. Thus, we can efficiently compute the scalar products and error indicators involving functions in different finite element spaces, like $\langle U_n - U_{n-1},\ V\rangle_\Omega$ or $\mathcal{E}^2_{c\tau}(U_n, U_{n-1}, \mathcal{G}_n)$.

5.2 *Coarsening*

At the beginning of each time-step we enlarge the time-step-size and coarsen the mesh from the previous time-step in the module `COARSEN`. As outlined in Remark 3.11 we double the actual time-step-size if the consistency error is sufficiently small.

Before describing the coarsening strategy actually used for the computations of Section 5.3, we recall that the error control of ASTFEM is principally independent of the coarsening employed. Thus, the simplest realization of coarsening would be to use $\mathcal{G}_{\text{init}}$ as an initial mesh and $T - t_{n-1}$ as initial time step size in each time step. This leads to meshes that are adapted very well to the stationary problem considered in any given time step. But then, the adaptive generation of the mesh $\mathcal{G}_n$ involves numerous iterations in Algorithm 2, which substantially increases the computation time. Moreover, also with respect to data oscillation (cf. Remark 3.4), a goal-oriented coarsening only aiming at removing as many *unneeded* degrees of freedom as possible seems appropriate. More precisely, given the solution $U_{n-1} \in \mathbb{V}(\mathcal{G}_{n-1})$ of the previous time step, a new grid $\mathcal{G}_* \leqslant \mathcal{G}_{n-1}$ is generated such that $|||U_{n-1} - I_* U_{n-1}|||_\Omega$ is small for some interpolation or projection operator $I_*\colon \mathbb{V}(\mathcal{G}_{n-1}) \to \mathbb{V}(\mathcal{G}_*)$; see Remark 3.11. We particularly employ the Lagrange interpolation operator as a realization of I_* since it can be implemented very efficiently. Exploiting on top of this a hierarchical mesh structure, as used in ALBERTA, it is relatively easy to compute the coarsening indicators $|||U_{n-1} - I_* U_{n-1}|||_\omega$ on suitable patches built from a collection of elements, which in turn gives rise to multiple coarsenings $\mathcal{G}_*$ of the mesh $\mathcal{G}_{n-1}$. In doing this, local hierarchy information given by the binary trees can be used to compute coarsening error indicators also for nonleaf tree elements. A combined coarsening of two elements corresponds to cutting two leaves off the corresponding tree. If repeated coarsening is allowed, whole subtrees may be cut off (cf. Möller, 2010).

5.3 *Numerical experiments*

In the two numerical examples presented here we consider equation (1.1) in the form of the plain heat equation, i.e., $\mathbf{A} = \mathrm{id}$, $c = 0$, on the time interval $(0, 1)$ and the spatial domain $\Omega = (-1, 1)^2 \subset \mathbb{R}^2$.

5.3.1 *Moving peak.* We take the example from Chen & Feng (2004, Section 5) by choosing the right-hand side f, the boundary condition and the initial value u_0 such that the exact solution is given by

$$u(x,t) = \alpha(t) e^{-\beta((x_1 - t + 0.5)^2 + (x_2 - t + 0.5)^2)} \quad \text{with } \alpha(t) = 1 - e^{-\gamma(t-0.5)^2}$$

and parameters $\beta = 25$ and $\gamma = 10^4$. The graph of u is an exponential peak moving at constant speed across the domain Ω. The peak experiences a rapid exponential drop around time $t = 0.5$ where it flattens to $u(x, 0.5) \equiv 0$. After this drop, the peak recovers as fast as it dropped and continues its uniform movement. This particular example allows us to examine various aspects of adaptivity. Besides that we also use this example to compare ASTFEM to a variant of the algorithm given by Chen & Feng

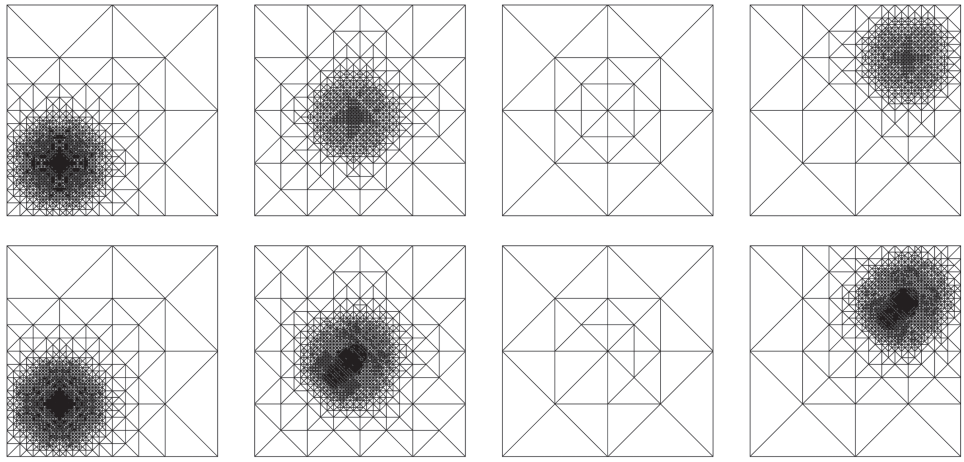

FIG. 1. Adapted meshes generated by ASTFEM (top) and CLASSIC (bottom) for times $t = 0$, $t \approx 0.49$, $t \approx 0.50$ and $t \approx 1.00$ (left to right).

(2004). We will refer to this algorithm as CLASSIC and the results presented here for CLASSIC are in agreement with those given in Chen & Feng (2004, Section 5).

We choose $\tau_0 = 10^{-3}$ as initial time-step-size and $\delta = 0.5$ as factor for decreasing the time-step-size. The employed tolerances are $\mathrm{TOL}_0^2 = 2.5 \times 10^{-6}$, $\mathrm{TOL}_f^2 = 2.5 \times 10^{-3}$ and $\mathrm{TOL}_{\mathcal{G}_\tau}^2 = 5 \times 10^{-3}$. We set $\mathrm{TOL}_*^2 = 2.5 \times 10^{-3}$, implying a minimal time-step size $\tau_* = 7.78 \times 10^{-7}$ using (3.13). As a marking strategy we use the maximum strategy with threshold parameter $\theta = 0.95$ for the generation of the initial mesh and $\theta = 0.8$ for the `MARK_REFINE` modules. The algorithm CLASSIC requires individual tolerances for the space and time error estimators. For this we split $\mathrm{TOL}_{\mathcal{G}_\tau}$ equally and use an additional coarsening tolerance $\mathrm{TOL}_{\mathrm{coarse}} = 3 \times 10^{-5}$.

The adaptive meshes generated by ASTFEM are displayed in Fig. 1 (top). We see that the spatial adaptivity captures the shape of the peak well by locally refining the mesh at the current position of the peak. We further note that the mesh is coarsened after the peak has passed by. Together with the observation that the mesh is nearly coarsened back to $\mathcal{G}_{\mathrm{init}}$ at $t = 0.5$, this shows that coarsening performs well.

Figure 2 shows that the temporal adaptivity detects the uniform behaviour in time away from $t = 0.5$ and produces a constant time-step size, which is only reduced to resolve the collapse of the solution around $t = 0.5$.

We particularly point out that the smallest time-step size actually employed in ASTFEM is much bigger than the threshold τ_* and we conclude that the nonstandard exit of the module `ST_ADAPTATION` is not used. In view of this, τ_* serves as a theoretical tool for guaranteeing termination within tolerance but does not influence the algorithmic flow in this example.

We next compare the two algorithms ASTFEM and CLASSIC. Figure 1 (bottom) depicts the adapted meshes produced by CLASSIC at (nearly) the same times as the meshes generated by ASTFEM. We observe that CLASSIC also captures the movement of the peak and its flattening around $t = 0.5$ well, and produces meshes that are quite similar to the meshes generated by ASTFEM even though they are finer. This is confirmed in Fig. 3 showing the number of degrees of freedom versus time and CPU time versus time. We also realize that the meshes of CLASSIC exhibit a slight trail in the opposite direction to the movement of the peak. This characteristic appears in a significantly weaker form in ASTFEM, which

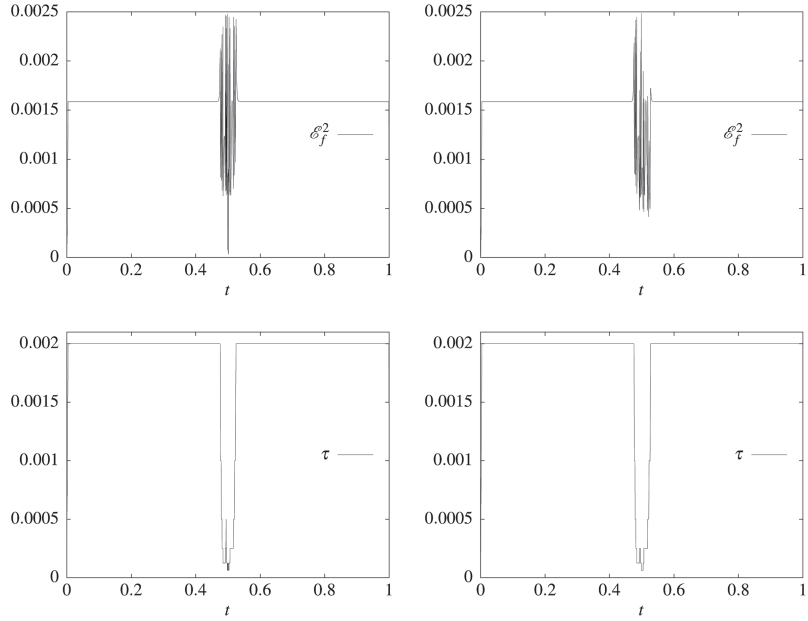

FIG. 2. Consistency error (top) and corresponding time-step sizes (bottom) produced by ASTFEM (left) and CLASSIC (right).

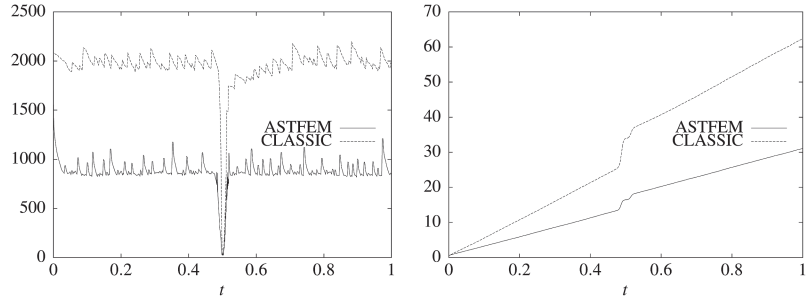

FIG. 3. Number of degrees of freedom in ASTFEM and CLASSIC (left) together with CPU time used in seconds on an AMD Opteron 252 at 2.6 GHz with 8 GB RAM (right).

is an indication that the coarsening of ASTFEM works more efficiently. The total sum of the space–time estimator is 4.69×10^{-3} for ASTFEM and 2.44×10^{-3} for CLASSIC. We would like to remark that in contrast to ASTFEM the space–time estimator for CLASSIC does not include the coarsening error, which we did not record explicitly. In view of this, the total space–time estimator for CLASSIC is larger than the stated value.

Figure 2 shows that the consistency error behaves almost identically for both algorithms. The total consistency estimators for both algorithms of approximately 1.57×10^{-3}. We point out that in this example the time-step size is exclusively controlled by the consistency indicator. More precisely, `CONSISTENCY` generates a time-step size that leads to $\mathcal{E}_{c\tau}$ being one magnitude smaller than $\mathcal{E}_f$. This implies a substantial waste of tolerance in CLASSIC since this algorithm employs a dedicated tolerance for the time error that is not exhausted by the small indicator $\mathcal{E}_{c\tau}$. Opposed to that, ASTFEM only aims at controlling the sum of space and coarsening–time error and thus implicitly allows for a bigger

space indicator. This adaptation according to the accumulated error indicator can be seen in Fig. 4. Since ASTFEM implicitly allows for a bigger space error, it employs fewer degrees of freedom. Consequently, ASTFEM is significantly faster than CLASSIC. Both features are depicted in Fig. 3.

5.3.2 *Rough initial data.* We conclude by an example with homogeneous Neumann boundary conditions and rough initial data, i.e., $u_0 \in L^2(\Omega)$ but $u_0 \notin H^1_0(\Omega)$. More precisely, we use a load function $f \equiv 0$ and as initial data a checkerboard pattern over $\Omega = (-1,1)^2$, i.e., u_0 is given by $u_0 \equiv 1$ in $\Omega_1 := (-1,0) \times (0,1) \cup (0,1) \times (-1,0)$ and $u_0 \equiv 0$ in $\Omega \setminus \Omega_1$. As an approximation $U_0 \in \mathbb{V}(\mathcal{G}_0)$, we use the L^2-projection $\Pi_0 u_0$, where $\mathcal{G}_0$ is adaptively constructed such that $\|U_0 - u_0\|^2_\Omega \leqslant \mathrm{TOL}_0^2 = 10^{-3}$. The other tolerances used by ASTFEM are set to $\mathrm{TOL}^2_{\mathcal{G}_\tau} = \mathrm{TOL}^2_* = 10^{-1}$.

We stress that rough initial data are included in our theory. In the crucial energy estimate of Proposition 3.6, only $|\!|\!| U_0 |\!|\!|_\Omega$ enters rather than $|\!|\!| u_0 |\!|\!|_\Omega$. After adaptively constructing U_0 we obtain from $|\!|\!| U_0 |\!|\!|^2_\Omega \approx 1\,813$ a minimal time-step size $\tau_* = 5.52 \times 10^{-6}$ by (3.13). Note that for such initial data, τ_* decreases when TOL_0 is reduced. We use $\tau_0 = \tau_*$ as an initial guess for the time-step size, which seems to be appropriate in this example.

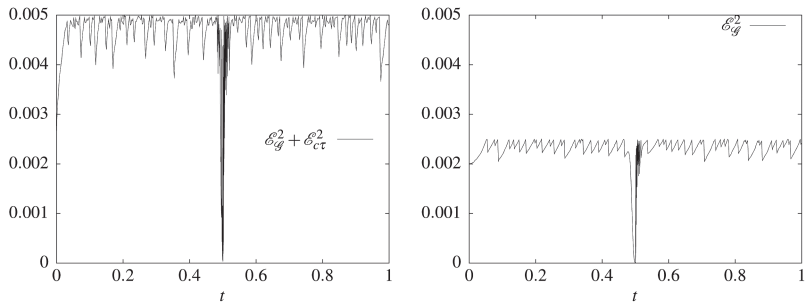

FIG. 4. Adapted quantity of ASTFEM (left) and space error estimator of CLASSIC (right).

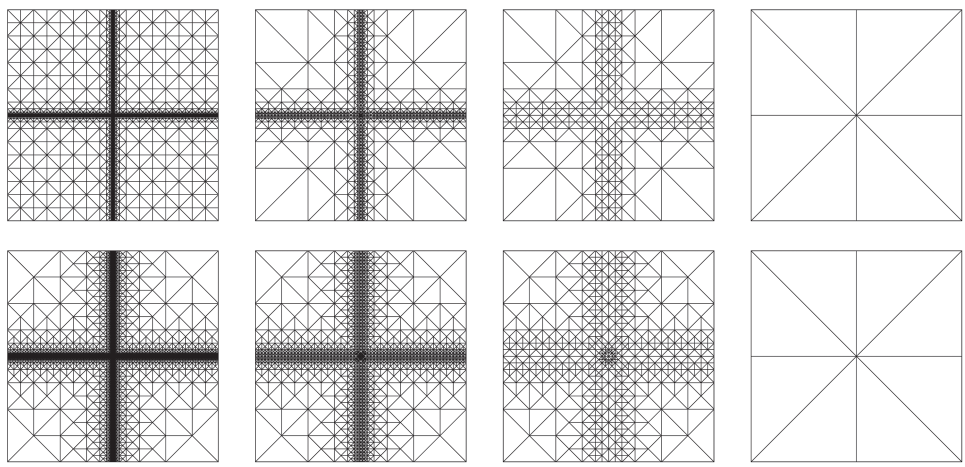

FIG. 5. Adapted meshes generated by ASTFEM at times $t = 0$, $t \approx 7.1 \times 10^{-4}$, $t \approx 5.6 \times 10^{-3}$, $t \approx 3.6 \times 10^{-1}$ (top) and CLASSIC at times $t \approx 6.7 \times 10^{-10}$, $t \approx 6.7 \times 10^{-4}$, $t \approx 6.0 \times 10^{-3}$, $t \approx 3.6 \times 10^{-1}$ (bottom). The initial grid $\mathcal{G}_0$ is the same for both algorithms (top left) and CLASSIC needs a high resolution in the first time step (bottom left).

During evolution, the jumps of u_0 are smoothed out and the solution u converges to the steady state $\bar{u} \equiv 0$ as $t \to \infty$. At final time $T = 1$ the exact solution is already close to the steady state but still away from it. In Fig. 5 (top) we depict the adaptive meshes generated by ASTFEM for different time instances from left to right starting with $\mathcal{G}_0$. The jumps of u_0 are resolved well over $\mathcal{G}_0$ by a strong refinement along the axes $x_1 = 0$ and $x_2 = 0$. As time passes, the smoothing is well reflected in the adaptively-generated meshes exhibiting an ongoing coarsening, particularly around the coordinate axes. Correspondingly, Fig. 6 (left) shows the effect of coarsening in terms of degrees of freedom.

Initially, ASTFEM makes use of the nonstandard exit in `ST_ADAPTATION`. This means that the time-step sizes are held constant at the minimal time-step size $\tau_* = 5.52 \cdot 10^{-6}$ until about $t = 2.8 \times 10^{-5}$. After this point the time-step size is being steadily enlarged as one expects; compare with Fig. 7 (left). The special treatment of these initial time steps is also reflected in the fact that the sum of space and coarsening–time error indicators exceeds its granted tolerance $\mathrm{TOL}^2_{\mathcal{G}_\tau} = 10^{-1}$; see Fig. 7 (right). We point out that summing the error indicators we get 1.56×10^{-3} as the value of the total space–time estimator. This clearly falls below the demanded total tolerance of $\mathrm{TOL}_0^2 + T\,\mathrm{TOL}^2_{\mathcal{G}_\tau} + \mathrm{TOL}_*^2 = 2.01 \times 10^{-1}$.

We finally briefly compare the performance of ASTFEM and CLASSIC, the latter one run with tolerances $\mathrm{TOL}_0^2 = 1.0 \times 10^{-3}$ and $\mathrm{TOL}^2_{\mathrm{space}} = \mathrm{TOL}^2_{\mathrm{time}} = \mathrm{TOL}^2_{\mathrm{coarse}} = 5.0 \times 10^{-2}$. The adaptive grids of CLASSIC are displayed in Fig. 5 (bottom). In this particular example ASTFEM completely outperforms CLASSIC for the following reasons. The initial time-step size accepted by CLASSIC is $\tau_1 \approx 6.71 \times 10^{-10}$, which is approximately 4 orders of magnitudes smaller than the inital time-step sizes τ_* used by ASTFEM. This in turn triggers additional refinements of the spatial grid resulting in

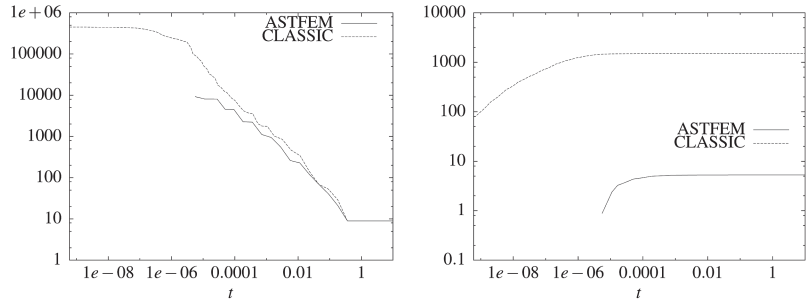

FIG. 6. Number of degrees of freedom in ASTFEM and CLASSIC (left) together with used CPU time in seconds on an AMD Opteron 252 at 2.6 GHz with 8 GB RAM (right).

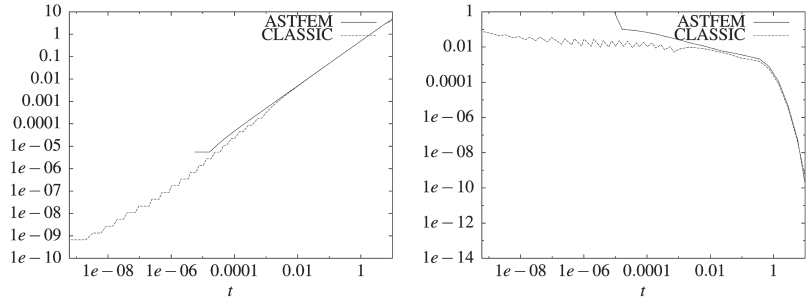

FIG. 7. Time-step sizes produced by ASTFEM and CLASSIC (left) and local error indicators $\mathcal{E}^2_{\mathcal{G}} + \mathcal{E}^2_{c\tau}$ for ASTFEM and CLASSIC (right).

449 877 elements compared to 9 293 elements generated by ASTFEM. After some time CLASSIC then also constantly enlarges the time-step sizes and coarsens the corresponding grids; compare with the history of time-step sizes in Fig. 7 (left), the adaptive grids in Fig. 5 (bottom), and the evolution of the degrees of freedom shown in Fig. 6 (left). In total, the space–time estimator sums up to 2.11×10^{-3}, which again does not include the coarsening error. Obviously, the much smaller time-step sizes and the much finer grids in the initial phase of CLASSIC have a strong impact on computation time. A comparison of CPU times is plotted in Fig. 6 (right), which shows that ASTFEM has terminated at end time before CLASSIC finalizes the first time step.

Acknowledgement

The second author gratefully acknowledges the support of the TUM Graduate School's Thematic Graduate Center TopMath at the Technische Universität München.

Funding

DFG research grant (SI-814/4-1) 'Adaptive Finite Elements for Parabolic PDEs' to K.G.S.

References

AINSWORTH, M. & ODEN, J. T. (2000) *A Posteriori Error Estimation in Finite Element Analysis*. New York: Wiley-Interscience.

BÄNSCH, E. (1991) Local mesh refinement in 2 and 3 dimensions. *IMPACT Comput. Sci. Eng.*, **3**, 181–191.

BINEV, P., DAHMEN, W. & DEVORE, R. (2004) Adaptive finite element methods with convergence rates. *Numer. Math.*, **97**, 219–268.

BINEV, P., DAHMEN, W., DEVORE, R. & PETRUSHEV, P. (2002) Approximation classes for adaptive methods. *Serdica Math. J.*, **28**, 391–416. Dedicated to the memory of Vassil Popov on the occasion of his 60th birthday.

CASCÓN, J. M., KREUZER, C., NOCHETTO, R. H. & SIEBERT, K. G. (2008) Quasi-optimal convergence rate for an adaptive finite element method. *SIAM J. Numer. Anal.*, **46**, 2524–2550.

CHEN, Z. & FENG, J. (2004) An adaptive finite element algorithm with reliable and efficient error control for linear parabolic problems. *Math. Comput.*, **73**, 1167–1193.

DIENING, L. & KREUZER, C. (2008) Convergence of an adaptive finite element method for the p-Laplacian equation. *SIAM J. Numer. Anal.*, **46**, 614–638.

DÖRFLER, W. (1996) A convergent adaptive algorithm for Poisson's equation. *SIAM J. Numer. Anal.*, **33**, 1106–1124.

ERIKSSON, K. & JOHNSON, C. (1991) Adaptive finite element methods for parabolic problems I: a linear model problem. *SIAM J. Numer. Anal.*, **28**, 43–77.

ERIKSSON, K. & JOHNSON, C. (1995) Adaptive finite element methods for parabolic problems II: optimal error estimates in $L_\infty L_2$ and $L_\infty L_\infty$. *SIAM J. Numer. Anal.*, **32**, 706–740.

EVANS, L. C. (1998) *Partial Differential Equations*. Graduate Studies in Mathematics, vol. 19. Providence, RI: American Mathematical Society.

GILBARG, D. & TRUDINGER, N. S. (2001) *Elliptic Partial Differential Equations of Second Order*. Classics in Mathematics. Berlin: Springer. Reprint of the 1998 edition.

KOSSACZKÝ, I. (1994) A recursive approach to local mesh refinement in two and three dimensions. *J. Comput. Appl. Math.*, **55**, 275–288.

KREUZER, C. & SIEBERT, K. G. (2011) Decay rates of adaptive finite elements with Dörfler marking. *Numer. Math.*, **117**, 679–716.

LAKKIS, O. & MAKRIDAKIS, C. (2006) Elliptic reconstruction and a posteriori error estimates for fully discrete linear parabolic problems. *Math. Comput.*, **75**, 1627–1658.

MAUBACH, J. M. (1995) Local bisection refinement for N-simplicial grids generated by reflection. *SIAM J. Sci. Comput.*, **16**, 210–227.

MEKCHAY, K. & NOCHETTO, R. H. (2005) Convergence of adaptive finite element methods for general second order linear elliptic PDEs. *SIAM J. Numer. Anal.*, **43**, 1803–1827.

MÖLLER, C. A. (2010) Adaptive finite elements in the discretization of parabolic problems. *Ph.D. Thesis*, Math. Nat. Fakultät, Universität Augsburg, Augsburg.

MORIN, P., NOCHETTO, R. H. & SIEBERT, K. G. (2000) Data oscillation and convergence of adaptive FEM. *SIAM J. Numer. Anal.*, **38**, 466–488.

MORIN, P., NOCHETTO, R. H. & SIEBERT, K. G. (2002) Convergence of adaptive finite element methods. *SIAM Rev.*, **44**, 631–658.

MORIN, P., NOCHETTO, R. H. & SIEBERT, K. G. (2003) Local problems on stars: a posteriori error estimators, convergence, and performance. *Math. Comput.*, **72**, 1067–1097.

MORIN, P., SIEBERT, K. G. & VEESER, A. (2008) A basic convergence result for conforming adaptive finite elements. *Math. Models Methods Appl.*, **18**, 707–737.

NOCHETTO, R. H., SIEBERT, K. G. & VEESER, A. (2009) Theory of adaptive finite element methods: an introduction. *Multiscale, Nonlinear and Adaptive Approximation* (R. A. DeVore & A. Kunoth eds). Berlin: Springer, pp. 409–542.

PETZOLDT, M. (2001) Regularity and error estimators for elliptic equations with discontinuous coefficients. *Ph.D. Thesis*, FU Berlin.

PETZOLDT, M. (2002) A posteriori error estimators for elliptic equations with discontinuous coefficients. *Adv. Comput. Math.*, **16**, 47–75.

SCHMIDT, A. (2003a) A multi-mesh finite element method for 3d phase field simulations. *Free Boundary Problems* (P. Colli, C. Verdi & A. Visintin eds). International Series of Numerical Mathematics, vol. 147. Basel: Birkhäuser, pp. 293–301.

SCHMIDT, A. (2003b) A multi-mesh finite element method for phase field simulations. *Interface and Transport Dynamics—Computational Modelling* (M. S. H. Emmerich & B. Nestler eds). Lecture Notes in Computational Science and Engineering, vol. 32. Berlin: Springer, pp. 208–217.

SCHMIDT, A. & SIEBERT, K. G. (2005) *Design of Adaptive Finite Element Software. The Finite Element Toolbox ALBERTA*. Lecture Notes in Computational Science and Engineering, vol. 42. Berlin: Springer.

SCHMIDT, A., SIEBERT, K. G., HEINE, C.-J., KÖSTER, D. & KRIESSL, O. (2005) *ALBERTA: An Adaptive Hierarchical Finite Element Toolbox*. Available at: http://www.alberta-fem.de/. Versions 1.2 and 2.0.

SCHWAB, C. & STEVENSON, R. (2009) Space–time adaptive wavelet methods for parabolic evolution problems. *Math. Comput.*, **78**, 1293–1318.

SIEBERT, K. G. (2011) A convergence proof for adaptive finite elements without lower bound. *IMA J. Numer. Anal.*, **31**, 914–946.

STEVENSON, R. (2007) Optimality of a standard adaptive finite element method. *Found. Comput. Math.*, **7**, 245–269.

TRAXLER, C. T. (1997) An algorithm for adaptive mesh refinement in n dimensions. *Computing*, **59**, 115–137.

VERFÜRTH, R. (1996) A review of a posteriori error estimation and adaptive mesh-refinement techniques. *Adv. Numer. Math.*, Chichester, UK: John Wiley.

VERFÜRTH, R. (1998) Robust a posteriori error estimators for a singularly perturbed reaction–diffusion equation. *Numer. Math.*, **78**, 479–493.

VERFÜRTH, R. (2003) A posteriori error estimates for finite element discretizations of the heat equation. *Calcolo*, **40**, 195–212.

VERFÜRTH, R. (2005) Robust a posteriori error estimates for nonstationary convection–diffusion equations. *SIAM J. Numer. Anal.*, **43**, 1783–1802.